St. John Fisher University

Fisher Digital Publications

2-15-2020

Effects of compaction pressure, speed and punch head profile on the ultrasonically-extracted physical properties of pharmaceutical compacts

Xiaochi Xu
Clarkson University

Yigitcan Coskunturk
Clarkson University

Vivek S. Dave
St. John Fisher University, vdave@sjf.edu

Justin V. Kuriyilel
St. John Fisher University, jvk09492@students.sjf.edu

Murray F. Wright
St. John Fisher University, mfw04071@students.sjf.edu

Publication Information

Effects of compaction pressure, speed and punch head profile on the ultrasonically-extracted physical properties of pharmaceutical compacts

Abstract

Despite a well-established manufacturing-process understanding, tablet quality issues are frequently encountered during various stages of drug-product development. Compact breaking force (tensile strength), capping and friability are among the commonly observed characteristics that determine the integrity, quality and manufacturability of tablets. In current study, a design space of the compaction pressure, compaction speed and head flat types is introduced for solid dosage compacts prepared from pure silicified microcrystalline cellulose, a popular tableting excipient. In the reported experiments, five types of head flat types at six compaction pressure levels and two compaction speeds were employed and their effects on compact mechanical properties evaluated. The mechanical properties of the tablets were obtained non-destructively. It is demonstrated these properties correlate well with compact porosity and tensile strength, thus their availability is of practical value. The reported mechanical properties are observed to be linearly sensitive to the tableting speed and compaction pressure, and their dependency on the head-flat profile, while clearly visible in the presented waveforms, was found to be nonlinear in the range of the parameter space. In this study, we detail a non-destructive, easy-to-use approach for characterizing the porosity and tensile strength of pharmaceutical tablets.

Keywords

fsc2020

Disciplines

Pharmacy and Pharmaceutical Sciences

Comments

Creative Commons License

Authors

Xiaochi Xu, Yigitcan Coskunturk, Vivek S. Dave, Justin V. Kuriyilel, Murray F. Wright, Rutesh H. Dave, and Centin Cetinkaya

Journal Pre-proofs

Effects of Compaction Pressure, Speed and Punch Head Profile on the Ultrasonically-Extracted Physical Properties of Pharmaceutical Compacts

Xiaochi Xu, Yigitcan Coskunturk, Vivek S. Dave, Justin V. Kuriyilel, Murray F. Wright, Rutesh H. Dave, Cetin Cetinkaya

Please cite this article as: X. Xu, Y. Coskunturk, V.S. Dave, J.V. Kuriyilel, M.F. Wright, R.H. Dave, C. Cetinkaya, Effects of Compaction Pressure, Speed and Punch Head Profile on the Ultrasonically-Extracted Physical Properties of Pharmaceutical Compacts, *International Journal of Pharmaceutics* (2019), doi: https://doi.org/10.1016/j.ijpharm.2019.118993

Effects of Compaction Pressure, Speed and Punch Head Profile on the Ultrasonically-Extracted Physical Properties of Pharmaceutical Compacts

Xiaochi Xu[1], Yigitcan Coskunturk[1], Vivek S. Dave[2], Justin V. Kuriyilel[2],

Murray F. Wright[2], Rutesh H. Dave[3] and Cetin Cetinkaya[1]*

[1] Photo-Acoustics Research Laboratory
Department of Mechanical and Aeronautical Engineering
Clarkson University
Potsdam, NY 13699-5725, USA

[2]St. John Fisher College
Wegmans School of Pharmacy
Rochester, NY 14618, USA

[3]Department of Pharmaceutical Sciences
Arnold and Marie Schwartz College of Pharmacy and Health Sciences
LIU-Natoli Institute
Long Island University
Brooklyn, NY 11201, USA

December 17, 2019

Version 02.02

*Corresponding author

8 Clarkson Ave. CAMP 241 Box 5725

Potsdam, NY 13699-5725

E-mail: cetin@clarkson.edu   Phone: (315) 268-6514   Fax: (315) 268 6695

Abstract

Despite a well-established manufacturing-process understanding, tablet quality issues are frequently encountered during various stages of drug-product development. Compact breaking force (tensile strength), capping and friability are among the commonly observed characteristics that determine the integrity, quality and manufacturability of tablets. In current study, a design space of the compaction pressure, compaction speed and head flat types is introduced for solid dosage compacts prepared from pure silicified microcrystalline cellulose, a popular tableting excipient. In the reported experiments, five types of head flat types at six compaction pressure levels and two compaction speeds were employed and their effects on compact mechanical properties evaluated. The mechanical properties of the tablets were obtained non-destructively. It is demonstrated these properties correlate well with compact porosity and tensile strength, thus their availability is of practical value. The reported mechanical properties are observed to be linearly sensitive to the tableting speed and compaction pressure, and their dependency on the head-flat profile, while clearly visible in the presented waveforms, was found to be nonlinear in the range of the parameter space. In this study, we detail a non-destructive, easy-to-use approach for characterizing the porosity and tensile strength of pharmaceutical tablets.

Keywords:

1. INTRODUCTION

Tablets are still the most popular dosage forms worldwide. Tablets owe their popularity to historical experience and convenience with manufacturing technology, ease of storage and handling, relatively better stability (physical, chemical, and biological), and greater patient compliance (Dave et al., 2017b). Despite a well-established manufacturing-process understanding, tablet quality issues are frequently encountered during various stages of drug-product development (early development, scale-up and production). Compact breaking force (ultimate tensile strength), capping/lamination and friability are among the commonly observed characteristics that determine the integrity and manufacturability of compacts (Dave et al., 2017a, 2015).

The mechanical properties, structural integrity and performance repeatability of compacts could be critical to its medical and other functions. The irregularities, defect and imperfections in a compact may compromise its physical and therapeutic properties/functions. Surface imperfections could adversely affect the efficacy of tablet coatings serving several objectives, such as regulating the release of therapeutic ingredients in the gastrointestinal tract, safeguarding the stability of its contents, and prolonging its shelf life. These types of defects are often related to (i) quality of raw materials, (ii) tablet production variables, and (iii) handling unit operations for processing, transport, and distribution. Subsequently, imperfections may also be taken as early indicators for shortcomings of production units, starting/incoming raw materials, and production parameters. Consequently, monitoring and testing compacts for irregularities, defect and imperfections is critical to the pharmaceutics sector for production performance and quality control/assurance objectives (Ilgaz Akseli et al., 2009).

A variety of formulation, process, and equipment variables influence the physical-mechanical properties of tablets. Avoiding these manufacturing related issues requires a thorough understanding and optimizing of these variables. Often there is less flexibility in changing formulation after being finalized and optimizing equipment/process factors becomes more important. The efficiency and success of a tablet compression process is largely determined by the turret diameter and speed, dimensions of pre-compression and compression rolls, and the tooling head (punches) profiles (Sinka et al., 2009). Particle rearrangement, fragmentation, and plastic deformation are primary mechanisms of powder compression (Nyström et al., 1993; Roberts and Rowe, 1987). Three stages broadly define the time-dependent process of tablet compression (e.g., compression, *compaction*, and *decompression stages*). The mechanical strength of a tablet is mainly determined by the compression force, but is material dependent and may lead to capping and lamination beyond a compressibility threshold.

It has long been known that compact mechanical strength can be improved by increasing the dwell-time of powder under maximum compression. Dwell-times can be increased by lowering turret speed, using a compression roll with larger diameter, and/or using tooling with wider head flat profiles (Anbalagan et al., 2017; Roberts and Rowe, 1985). Among these, utilizing punches with optimal head-flat diameters is observed to be a more convenient approach to manufacture strong compacts. During a tableting cycle, the flat region of the tooling head profile determines the ideal maximum compaction effect without any vertical displacement. The diameter of this flat surface thus determines the dwell-time, and subsequently the mechanical strength of the compact. Currently, tablet tooling with a wide range of diameters are available commercially.

Previously we introduced and reported a number of a non-destructive/non-invasive, acoustic wave propagation-based methods for the testing and characterization of compact properties (Varghese and Cetinkaya, 2007; I. Akseli et al., 2009; Ilgaz Akseli et al., 2009; Liu and Cetinkaya, 2010; Smith et al., 2011; Vahdat et al., 2013). Current literature reveals limited information on the influence of tooling head-flat geometry on the mechanical properties of compacts. A recent study reported the effects of punch head geometry on the quality of compacts prepared on a tablet press (Anbalagan et al., 2017). In their study, these researchers studied the effects of punch head diameters and compression roll design on the compressibility of a paracetamol formulation. The study results showed a minimal effect of punch head-flat diameter on the compression profile of the formulation, and non-significant effects on the mechanical properties of compacts. Recently, our laboratory evaluated two direct compression guaifenesin formulations with different drug loading to analyze the effects of punch head-flat diameters and tooling type (i.e., B or D) on the mechanical/physical properties of compacts (Shah et al., 2019). In this study, we observed that punch head geometry had some influence on the tensile strength, albeit this effect was dependent on tooling size used (B or D). Moreover, the punch head profile was also found to be responsible for the incidences of 'capping' phenomena observed in the compacts. The studies mentioned above utilized a prototype formulation containing a drug and one or more excipients. Using a single-component material can theoretically provide a more accurate estimation of the effects of tooling head-flat diameter on the mechanical properties of tablet samples.

Thus to further explore this phenomena, in the current work we explored the effects of tooling head-flat diameter on the mechanical properties of compacts at various compaction pressures and compaction speeds using a popular tableting excipient Prosolv® SMCC 90LM (silicified

6

microcrystalline cellulose) as a model material. Furthermore, we explored the feasibility of correlating the acoustically extracted information the mechanical properties of these compacts.

The specific objectives of the reported study include:

- Extract the key mechanical properties (c_L, c_T and E_A) of the compact materials from acquired acoustic waveforms in a non-destructive manner,

- Analyze the effects of the tooling head-flat diameter, compaction speed (dwell-time) and force (pressure) on the compact mechanical and ultrasonic properties at a range of compaction pressure and speed (dwell-time) levels, and

- Correlate the acoustically obtained parameters with the key physically measured mechanical properties of the tablets (compact porosity and tensile strength).

2. MATERIALS AND METHODS

2.1 Tablet Manufacturing

For current study, a number of compacts of the Prosolv® SMCC 90LM (silicified microcrystalline cellulose) were pressed on an instrumented, single-layer, rotary compaction press with ten stations (Piccola B-506, SMI Inc., Lebanon, New Jersey, USA) using 10 mm, flat faced, B tooling (SMI Inc., Lebanon, New Jersey, USA). In producing sample tablets, the target tablet mass was set at 400 mg. For each tooling type, five different types of head flats (HF) (i.e., No HF 50% HF, Standard HF, Extended HF, and 0.625 HF) with a diameter of 0, 4.78, 9.53, 13.34 and 15.89 mm on the head tips with a diameter of 25.36 mm, (Natoli Engineering Company, Inc.) were used to prepare the compacts (Fig. 1.a). The samples were prepared at two levels of tableting speed (v_c), (namely, 20 RPM (rotation per minute) and 50 RPM) and six levels of the compaction pressure

($P_1 - P_6$): 6.4, 15.9, 31.9, 47.8, 63.7, and 79.6 MPa, respectively. The tableting speed and the compaction pressures were acquired and monitored in real time with the help of the monitoring software tool (*the Director*, SMI Inc., Lebanon, New Jersey, USA). The true densities of the material was measured on a helium displacement pycnometer (AccuPyc$^®$ 1340, Micromeretics, Norcross, Georgia, USA) using the method included in the United States Pharmacopeia (USP) 38 – NF 33, general chapter <699> on the density of solids. These measurements were executed three times after equilibrating the material in a desiccator for over 24 hours.

2.2 Compact Sample Set

In current study, five types of cylindrical tablets (referred to as HF01, HF02, HF03, HF04 and HF05) were prepared with corresponding head flat profile types of No HF, 50% HF, Standard HF, Extended HF, and 0.625 HF, respectively (Table 1). Each sample set was compacted at two levels of compaction rates: corresponding to 4 milliseconds at high compaction speed (HS) and 20 milliseconds at low speed (LS) peak compaction dwell-times, respectively. The resulting ten data sets are referred to as LS_HF01, LS_HF02, LS_HF03, LS_HF04, LS_HF05 and HS_HF01, HS_HF02, HS_HF03, HS_HF04, HS_HF05, respectively. For each data set, six compaction pressure levels (P_1=6.4 MPa, P_2=15.9 MPa, P_3=31.9 MPa, P_4=47.8, P_5=63.7 and P_6=79.6 MPa) are exerted. In Table 1, the complete set of measured tablet properties (e.g., thicknesses, diameters, weights, mass densities, average compact porosity and ultimate tensile strength) are listed. Conseqeunty, a three-dimensional design space for six compaction force levels (P_1, P_2, P_3, P_4, P_5 and P_6) and five head flat types (HF01, 02, 03, 04, and 05) at two compaction speeds (high and low speeds) is created. Altogether, the complate sample set consists of 60 (5×2×6) types of experimental samples (compacts).

In current study, for each compaction type, twelve tablets (samples) were employed. The total number of tablets in the complete sample set was 720. In Table 1, the compact sizes measured by a digital caliper (CD-6 in CS Absolute Digimatic, Mitutoyo Inc., Aurora, Illinois, USA) with an error range of $\pm\,5\times10^{-6}$ m and masses obtained by a digital balance (A120S-L, Mettler-Toledo Inc., Columbus, Ohio, USA) with an error range of $\pm\,50$ micrograms are included.

2.3 Compact Evaluation

The mass porosity (ϕ^{m}) of the sample compact in percentage (%) was determined using the bulk (ρ_{b}) and true (ρ_{t}) densities of the compacts by:

$$\phi^{m}(\%) = \left(1 - \frac{\rho_{b}}{\rho_{t}}\right) \times 100 \tag{1}$$

Based on the method specified in USP38 – NF 33, general chapter <905> on the uniformity of dosage units, the mass variation of the samples was also evaluated. A set of compact (n=12) were arbitrarily sampled from each compact batch, and individually weighed. The breaking pressure (diametrical crushing strength) of the sample tablets was evaluated using the technique detailed in USP38 – NF33, *General Chapter<1217>: Tablet Breaking Force*. In the reported experiments, ten random samples from each sample batch were tested with a hardness tester (VK200, Varian, Inc., Cary, North Carolina, USA). The average ultimate tensile strength σ_{b}^{m} and porosity ϕ^{m} values of the test compacts are reported in Table 1.

2.4 Ultrasonic Waveform Acquisitions

In current study, an acoustic experimental test rig based on an ultrasonic characterization equipment (ATT2020, Pharmacoustics Technologies, LLC, Potsdam, New York, USA) was constructed and employed. In the current set-up, the ATT2020 instrument is configured with two pressure (compression) transducers (V540-SM, Olympus Corporation, Center Valley, PA, USA) with the central frequency of 2.25MHz, two shear (transverse wave) transducers (V154-RM, Olympus Corporation, Center Valley, PA, USA) with the central frequency of 1MHz, a pair of low attenuation delay-lines, an axial load monitoring system, and a tablet sample centering apparatus. The instrument is controlled by a GUI (graphical user interface) based on a data acquisition software (LabVIEW 15, National Instruments Corp., Austin, Texas, USA) for signal acquisition, storage and ToF analysis (Fig. 1.b). The ATT2020 tool can be operated in pulse-echo (reflection) or pitch-catch (transmission) modes for both pressure (longitudinal) and shear (transverse) waves.

In the reported pressure and shear work, the experimental rig was employed to acquire the ultrasonic transient responses (waveforms) for evaluating the macro-scale physical properties of the tablet materials. In the reported experiments, the ATT2020 tool was operated in pitch-catch mode in which the pulser-receiver parameters were set at a pulse width of 200 ns, a pulser voltage of 200 V, a sampling rate of 100 MHz, an amplification gain of 0 dB, and an averaging rate of 2^9. In the pressure measurement station (left apparatus in Fig. 1.b), the top transducer (Transducer 1) was coupled with a low-attenuation delay-line and mounted into the upper transducer holder. The bottom transducer (Transducer 2) was mounted into the bottom transducer/tablet holder. The surface contact between the transducer-tablet interfaces is secured for the maximum transmission

of propagating pulses. A load cell mounted at the bottom of each lower transducer holder platform and connected to its control unit with a display was used to report, monitor and save the applied axial force (on compact) during data acquisition. The exerted axial force eliminates the effects of surface asperities on ultrasonic waveform quality. In the reported experiments, the axial load was maintained at 1500 ± 10g for ensuring repeatable wave transmission contact between the compact and the faces of the delay-line and transducers. Compared to the compaction pressures P_c (P_1=6.4 MPa, P_2 =15.9 MPa, P_3 =31.9 MPa, P_4 =47.8 MPa, P_5 =63.7 MPa and P_6 =79.6 MPa), the applied axial force levels (a few N) are low, thus no substantial alteration on tablet deformation is anticipated. The exerted axial load level on each tablet sample is read, saved and displayed on the local display and/or the ATT2020 instrument GUI. In the transverse (shear) wave station (Fig. 1.b - right), the tool with shear transducers have the same configuration as the pressure station. In the shear experiments, an acoustic shear couplant gel (54-T04, Sonotech, Glenview, Illinois, USA) was utilized.

In the reported experiments in the pitch-catch mode, a sample compact was placed and centered on the bottom holder such a way that the bottom surface of the compact contacted with Transducer 2. Before data acquisition, each tablet was centered and fixed by an iris and the parallelism of the transducer faces was verified by a visual examination of the contact zone with a light source.

3. RESULTS AND DISCUSSIONS

In Fig. 2, the acquired waveforms for the five sample sets (HF01, HF02, HF03, HF04 and HF05) at each compaction pressure P_c level (P_1 = 6.4 MPa, P_2 = 15.9MPa, P_3 =31.9MPa, P_4 =47.8MPa, P_5 =63.7MPa and P_6 = 79.6MPa) with low and high compaction speed (LS and HS) are depicted.

In the pressure waveforms for the data sets with low compaction speed (LS_HF01, LS_HF02, LS_HF03, LS_HF04 and LS_HF05) (Fig. 2.a), it is observed that, with increasing P_c (from P_1 to P_6), the arrival times of pressure pulses shorten, which indicates the propagation speed (thus ToF) is sensitive to the compaction pressure P_c level. Note that the shifting trend was less evident at higher compaction pressure levels (P_4, P_5 and P_6). In addition, the arrival of pressure pulses vary between each sample set (LS_HF01, LS_HF02, LS_HF03, LS_HF04 and LS_HF05) at each compaction pressure level ($P_1 - P_6$), implying tooling head flat type effects on the pressure wave propagation velocity. In Fig. 2.b, a similar trend is noted for the sample sets with high compaction speed (HS_HF01, HS_HF02, HS_HF03, HS_HF04 and HS_HF05). This trend was observed for shear waveforms as well (Figs. 2.c-d). It is observed that the ToF of pressure and shear wave pulses is sensitive to P_c, which indicates the dwell-time (compaction speed) and force modifies the pressure and shear wave velocities (as clearly observed in Fig. 2).

The acquired pressure waveforms are processed to obtain ToF (Δt_L and Δt_T for the pressure and shear waves, respectively) determined by two time-frequency techniques (i.e, the short-term Fourier (STFT) and Gabor wavelet transforms). In extracting Δt_L and Δt_T in a dispersive material, a time-frequency technique is employed, which requires the ToF of strain energy at a particular frequency (not necessarily the amplitude of incoming wave pulses) (Drai et al., 2002). For a compact (with a thickness of h), the corresponding average pressure and shear wave speeds (c_L and c_T) are calculated as:

$$c_L = h / \Delta t_L \qquad c_T = h / \Delta t_T \qquad\qquad 2$$

From the extracted the wave speed c_L, the apparent Young's modulus of the material is determined by $E_A = c_L^2 \times \rho_A$, where ρ_A is the apparent mass density of the sample material. In Table 1, for the

sample sets (HF01, HF02, HF03, HF04 and HF05), the average measured compact thicknesses (h), diameters (d), masses (m), apparent mass densities (ρ_A), average value of the compact porosity (ϕ^m) and tensile strength (σ_b^m) from direct measurements, and the acoustically extracted parameters: pressure (c_L) and shear (c_T) wave speeds, average apparent Young's moduli (E_A) for the six levels of P_c ($P_1 = 6.4$ MPa, $P_2 = 15.9$MPa, $P_3 = 31.9$MPa, $P_4 = 47.8$MPa, $P_5 = 63.7$MPa and $P_6 = 79.6$MPa) are summarized.

As seen in Fig. 2, the reflections (peak values) of the compact samples shift to the left with the increasing values of compaction pressure P_c (from P_1 to P_6), indicating a reduction in the Δt_L and Δt_T values. The pressure wave ToF values for the tablet sample set LS-HF03 were obtained as Δt_L = 8.54, 4.24, 2.59, 2.09, 1.88 and 1.69μsec for each P_c, respectively (Fig. 2.a), which indicates that Δt_L and Δt_T is sensitive to P_c. In Fig. 2, it is also seen that the pressure arrivals of the tablet differ between the sample sets (HF01 – HF05) at each P_c level (implying a change in speeds), i.e. Δt_L = 8.66, 8.70, 8.54, 8.17 and 8.34 μsec for LS_HF01 – LS_HF05 (Fig. 2.a) at compaction level P_1, respectively. It is indicated that the ToF was modulated by the types of heat flat in a nonlinear manner. Moreover, the pressure wave arrivals of the tablets vary between low speed samples (LS_HF01-HS_HF06) and high speed samples (HS_HF01-HS_HF06) at each P_c level (implying a change in wave speed). For example, pressure Δt_L = 8.54, 4.24, 2.59, 2.09, 1.88 and 1.69 μsec in LS_HF03 and Δt_L = 8.60, 4.49, 2.74, 2.23, 1.99 and 1.89 μsec in HS_HF03 for each P_c, respectively.

Superimposed plots for c_L, c_T and E_A with a function of head flat type (HF01 – HF05) for each sample set at compaction pressure ($P_1 – P_6$) are presented in Fig. 3. It is observed that the c_L, c_T

13

and E_A curves for all the sample sets raise with an increase in P_c (P_1 - P_6), indicating pressure and shear wave speed (c_L and c_T) was strongly modulated by P_c. In Fig. 3, it is also observed that c_L, c_T and E_A value nonlinearly varies between head flat types (HF01 – HF05) at each P_c, this variation become more evident with an increase in P_c. Moreover, c_L, c_T and E_A curves for the sample set with low compaction speed (LS_HF01 – LS_HF05) are higher than those with high compaction speed (HS_HF01 – HS_HF05) at each P_c (Fig. 3). It is concluded that c_L, c_T and E_A curves are more sensitive to compaction pressure P_c and compaction speed v_c, less sensitive to head flat type (HF01-HF05).

3.1 Analysis of the Compact Mechanical Properties

Previously reported relationships, i.e. compressibility, tabletability, and compactibility, were used to analyze the mechanical performance of the prepared compacts. *Compressibility* is generally described as the extent of volume reduction by a material as a function of an applied axial force in a compaction die. This relationship is characterized by a chart of the compression pressure (defined as P_c/A_T) (A_T is the lateral cross-sectional area of the compact) *vs* calculated compact porosity. The plot of P_c versus σ_b^m is generally known as *Tabletability*. It is thought to be the ability of a pharmaceutical powder to form a compact of given tensile strength as a function of compression force. *Compactibility* relates two most important properties of a compact formed by compression: compact strength and compact porosity, and is considered to be the most practically useful parameter. Compactibility is represented as a correlation of a compact's tensile strength to its porosity. In principle, it represents the capacity of a powder bed to form a compact of a certain strength at a given solid fraction (density). The compressibility profiles of pure Prosolv® SMCC 90LM compressed using different tooling (HF01 – HF05) (Fig. 1.a), at low (LS) and high (HS)

14

speed are shown in Fig. 4.a-b. Usually, the compact porosity decreased in a non-linear manner with increasing compression pressures. For compacts prepared at low speed, the tooling head-flat design did not appear to significantly influence the compressibility of the material. At high speed compression, the porosity of the compacts prepared using different tooling overlapped at low compression pressures. However, at higher compression pressures, the compressibility profiles appeared to diverge. The lowest porosity was achieved by the material compressed using 0.625 HF tooling (HF05). This tooling has the widest head-flat diameter. While the effects are less pronounced, the observations agree with our hypothesis that a larger head-flat surface allows for a relatively longer dwell-time to a powder under compression, thus increasing its compressibility. The tableting speed did not appear to have an influence on the compressibility of Prosolv® SMCC 90LM. This finding was unexpected considering the fact that microcrystalline cellulose is generally known to be a plastically deforming material, and its mechanical properties are sensitive to compaction speeds. However, these observations could be attributed to the fact that Prosolv® SMCC 90LM is not pure MCC but a co-processed material containing silicone dioxide, and may deform *via* more than one mechanism. The tabletability profiles (compression pressure *vs.* compact tensile strength) of pure Prosolv® SMCC 90LM compressed using different tooling, at low (Fig. 4.c) and high (Fig. 4.d) compaction speeds are shown. Generally, the ultimate tensile strength of compacts increased with increasing pressures about ~50 MPa. Above this level, compact tensile strength appear to plateau. For compacts prepared at low speed, the tooling type had a marginal influence on the tensile strength, albeit only at lower compression pressures. At higher compression pressures the tensile strength of compacts overlapped for all tooling types. Similar results were observed for compacts prepared at higher speeds. The compactibility profiles (compact porosity *vs.* compact tensile strength) of pure Prosolv® SMCC 90LM compressed using

different tooling, at low (Fig. 5.a) and high (Fig. 5.b) compaction speed are shown below. Generally for a given material/formulation, the compactibility profiles are independent of compaction speeds. Moreover, compactibility is directly proportional to the compact solid fraction (inversely proportional to the compact porosity). For Prosolv® SMCC 90LM, the compactibility profiles followed the expected path. For compacts prepared at both high and low compaction speeds, the tooling head-flat design appeared to have an insignificant effect on the tablet compactibility, except at compact porosities around ~35%. At this porosity (corresponding to the compression pressure of ~50 MPa), the tensile strength of the compacts appeared to vary as a function of tooling type. However, this effect was not pronounced.

3.2 Correlation of the Compact Porosity ϕ^m with c_L, c_T, and E_A

One of the main goals of the presented work was to study the feasibility of correlating the measured mechanical attributes of the prepared compacts with the acoustically obtained parameters. Fig. 6.a shows the changes in the acoustic wave pressure velocities (c_L) as a function of measured compact porosities. It was observed that the pressure wave velocities were inversely proportional to the compact porosities, i.e. c_L was found to be lowest at the highest compact porosity, and increase proportionally with decreasing porosities. In addition, the c_L values clearly distinguished the sets of compacts prepared at different compression speeds. Compacts prepared at lower speeds exhibited higher c_L values compared to those prepared at higher speeds. For the compacts prepared at a given speed, c_L was unable to differentiate between different tooling head-flat geometries. In Fig. 6.b, the correlation levels between the porosities of tablet materials (ϕ^m) and the acoustically obtained shear wave speed (c_T) for all sample sets are presented and an inverse correlation was observed between ϕ^m and c_T in all sample sets. Note that the c_T values overlapped for the sets of

compacts prepared at low (LS) and high (HS) compression speeds. As expected, the c_T values of the compacts in the sample sets were observed to directly correlate with ϕ^m. In Fig. 6.c, the effect of porosities on the Young's moduli E_A of materials is demonstrated. The apparent Young's modulus is determined by $E_A = c_L^2 \times \rho_A$, where, ρ_A is the mass density of a compact. Similar to the observations above, the E_A values were found to be inversely proportional to compact porosities, i.e. lower E_A values were observed at higher porosities and *vice versa*. Furthermore, clear separation was observed between the E_A values obtained for sets of compacts prepared at different speeds. Compacts prepared at higher compression speeds exhibited lower E_A values and *vice versa*. E_A values for different tooling head-flat geometries within a set of compacts prepared at a given speed were not significantly different. Overall, these results establish sensitivity and correlation of the acoustic parameters to the measured physical-mechanical attributes of the compacts, and theoretically support the feasibility using acoustic measurements in predicting these attributes with relative accuracy.

3.3 Correlation of the Tensile Strength σ_b^m with c_L, c_T, and E_A

In line with the goals of current work, we also attempted to correlate the acoustically obtained parameters with the measured physical-mechanical properties of prepared compacts. The changes in acoustically obtained c_L and c_T values as a function of measured compact tensile strength were shown in Figs. 7.a-b. In general, c_L and c_T values were found to be directly proportional to the compact tensile strength, i.e. higher c_L and c_T values were observed for compacts with higher tensile strength, and *vice versa*. The c_L and c_T values correlated in a near-linear fashion with increasing compact tensile strength up to ~5 MPa, beyond which deviations were observed. Interestingly, the c_L and c_T values were unable to differentiate compacts prepared at different

compression speeds or between compacts prepared using different tooling head-flat geometries at a given speed for compacts with tensile strengths up to ~5 MPa. Beyond the compact tensile strength of 5 MPa, the c_L and c_T values appeared to be grouped based on the compression speed, i.e. higher values of c_L and c_T were observed for compacts prepared at lower speeds (LS) and *vice versa*. Fig. 7.c shows the influence of the compact tensile strength on the apparent Young's modulus. Similar to the observations above, the acquired Young's modulus appeared to be directly proportional to the compact tensile strength. However, Young's modulus calculated using acoustic parameters appeared to be less sensitive to the compression speeds or the tooling head-flat geometries.

5. CONCLUSIONS AND REMARKS

A design space of the compaction pressure (P_c), compaction speed (v_c) and head flat types (HF) is introduced for solid dosage compacts prepared from pure silicified microcrystalline cellulose, a popular tableting excipient (see Table 1 for the complete sample set information). In the reported experiments, five types of head flat (profile) types (No HF, 50% HF, Standard HF, Extended HF, and 0.625 HF) at six compaction pressure levels ($P_1 = 6.4$ MPa, $P_2 = 15.9$ MPa, $P_3 = 31.9$ MPa, $P_4 = 47.8$ MPa, $P_5 = 63.7$ MPa and $P_6 = 79.6$ MPa) and two dwell times v_c (4 and 20 milliseconds peak compression dwell-time, high (HS) and low (LS) speeds respectively) were employed and their effects on compact mechanical properties evaluated. The ultrasonic and physical properties of the tablets (c_L, c_T and E_A) were extracted non-destructively from their ultrasonic responses with the presented acoustic experimental mechanism. While the measured mechanical properties of the compacts appeared to be more sensitive to the tableting speed and compaction pressure, and less sensitive to the head-flat geometries, the reported acoustically obtained mechanical properties of the sample compacts are observed to correlate well to all the tableting speed (v_c) and compaction

18

pressure (P_c), and to the punch head profiles (HF). The reported properties are found to be linearly sensitive to the tableting speed and compaction pressure. While clearly visible in the presented waveforms, their dependency on the head-flat geometry was observed to be nonlinear in the range of the parameter space, thus requiring further investigation and analysis.

From the extracted ToF (Δt_L) results of the pressure wave propagation in the data sets, the pressure and shear wave speed (c_L and c_T) and Young's modulus (E_A) of the compact materials were determined and reported. It is noted that c_L, c_T and E_A values increase with increasing P_c, and become constant after a critical compression force value, indicating that the mechanical properties (c_L, c_T and E_A) and compaction pressure are in correlation. In addition, c_L, c_T and E_A value varies between head flat types (HF01 – HF05) at each P_c, this variation become more evident with increasing P_c. Moreover, c_L, c_T and E_A curves for the sample set with low compaction speed (LS_HF01 – LS_HF05) are higher than those with high compaction speed (HS_HF01 – HS_HF05) at each P_c. Overall, the sensitivity of the mechanical properties (c_L, c_T and E_A) of the tablets were found to be sensitive in a decreasing order to the compression pressure P_c, tableting speed v_c, and changes in tooling head flat profiles.

Here we present a powder and compression/compaction parameters based design space, and a non-destructive ultrasonic ToF technique for predicting the mechanical properties and tensile strength of pharmaceutical compacts in a non-destructive manner. The presented methodology can be adopted at various stages of materials processing research, product development and solid dosage production. For example, during pre-formulation and formulation stages, the physical/mechanical characterization of neat materials and complex (mixture) formulations is a crucial step. Also, by utilizing the presented approach, formulation development and scale-up scientists can optimize the formulation and process variables with minimal material loss. In tablet production, the technique

can lower the time durations required for product quality assurance, examinations and corrective actions in production lines.

In sum, the presented approach and characterization technique supports the QbD (Quality-by-Design)-PAT (Process Analytic Technology) paradigm of the U.S. FDA (United States Food and Drug Administration).

ACKNOWLEDGEMENTS

LIST OF REFERENCES

Akseli, Ilgaz, Becker, D.C., Cetinkaya, C., 2009. Ultrasonic determination of Young's moduli of the coat and core materials of a drug tablet. International journal of pharmaceutics 370, 17–25.

Akseli, I., Hancock, B.C., Cetinkaya, C., 2009. Non-destructive determination of anisotropic mechanical properties of pharmaceutical solid dosage forms. International journal of pharmaceutics 377, 35–44.

Anbalagan, P., Sarkar, S., Liew, C.V., Heng, P.W.S., 2017. Influence of the Punch Head Design on the Physical Quality of Tablets Produced in a Rotary Press. Journal of Pharmaceutical Sciences 106, 356–365. https://doi.org/10.1016/j.xphs.2016.10.016

Dave, V.S., Fahmy, R.M., Hoag, S.W., 2015. Near-infrared spectroscopic analysis of the breaking force of extended-release matrix tablets prepared by roller-compaction: influence of plasticizer levels and sintering temperature. Drug Dev Ind Pharm 41, 898–905. https://doi.org/10.3109/03639045.2014.911883

Dave, V.S., Popielarczyk, M., Boyce, H., Al-Achi, A., Ike-Amaechi, E., Hoag, S.W., Haware, R.V., 2017a. Lubricant-Sensitivity Assessment of SPRESS® B820 by Near-Infrared Spectroscopy: A Comparison of Multivariate Methods. J Pharm Sci 106, 537–545. https://doi.org/10.1016/j.xphs.2016.09.018

Dave, V.S., Shahin, H.I., Youngren-Ortiz, S.R., Chougule, M.B., Haware, R.V., 2017b. Emerging technologies for the non-invasive characterization of physical-mechanical properties of tablets. Int J Pharm 532, 299–312. https://doi.org/10.1016/j.ijpharm.2017.09.009

Drai, R., Khelil, M., Benchaala, A., 2002. Time frequency and wavelet transform applied to selected problems in ultrasonics NDE. NDT & E International 35, 567–572. https://doi.org/10.1016/S0963-8695(02)00041-5

Liu, J., Cetinkaya, C., 2010. Mechanical and geometric property characterization of dry-coated tablets with contact ultrasonic techniques. International journal of pharmaceutics 392, 148–155.

Nyström, C., Alderborn, Gör., Duberg, M., Karehill, P.-G., 1993. Bonding Surface area and Bonding Mechanism-Two Important Factors fir the Understanding of Powder Comparability. Drug Development and Industrial Pharmacy 19, 2143–2196. https://doi.org/10.3109/03639049309047189

Roberts, R.J., Rowe, R.C., 1987. Brittle/ductile behaviour in pharmaceutical materials used in tabletting. International Journal of Pharmaceutics 36, 205–209. https://doi.org/10.1016/0378-5173(87)90157-8

Roberts, R.J., Rowe, R.C., 1985. The effect of punch velocity on the compaction of a variety of materials. J. Pharm. Pharmacol. 37, 377–384. https://doi.org/10.1111/j.2042-7158.1985.tb03019.x

Shah, H.G., Dugar, R.P., Li, H., Dave, V.S., Dave, R.H., 2019. Influence of punch geometry (head-flat diameter) and tooling type ("B" or 'D') on the physical-mechanical properties of formulation tablets. Drug Dev Ind Pharm 45, 117–123. https://doi.org/10.1080/03639045.2018.1525395

Sinka, I.C., Motazedian, F., Cocks, A.C.F., Pitt, K.G., 2009. The effect of processing parameters on pharmaceutical tablet properties. Powder Technology, Special Issue: 3rd International Workshop on Granulation: Granulation across the Length Scales 189, 276–284. https://doi.org/10.1016/j.powtec.2008.04.020

Smith, C.J., Stephens, J.D., Hancock, B.C., Vahdat, A.S., Cetinkaya, C., 2011. Acoustic assessment of mean grain size in pharmaceutical compacts. International journal of pharmaceutics 419, 137–146.

Vahdat, A.S., Vallabh, C.K.P., Hancock, B.C., Cetinkaya, C., 2013. Ultrasonic approach for viscoelastic and microstructure characterization of granular pharmaceutical tablets. International journal of pharmaceutics 454, 333–343.

Varghese, I., Cetinkaya, C., 2007. Noncontact photo-acoustic defect detection in drug tablets. Journal of pharmaceutical sciences 96, 2125–2133.

Table 1. The measured compact thicknesses (h), diameters (d), masses (m), apparent mass

densities (ρ_A), tablet porosity (ϕ^m) and tensile strength (σ_b^m) are listed along with the acoustically

extracted parameters: c_L and c_T and corresponding Young's moduli (E_A) for the five sample sets

of tablets (i.e., HF01, HF02, HF03, HF04 and HF05) for the six levels of P_c.

Sample Set	Compaction Pressure P_c (MPa)	Measured Parameters						
		h (mm)	d (mm)	m_A (g)	ρ_A (kg/m³)	c_L (m/sec)	c_T (m/sec)	E_A (GPa)
HF01_LS	6.4	6.49 ± 0.03	10.10 ± 0.02	0.396 ± 0.001	763.11 ± 3.24	748.60 ± 11.99	525.51 ± 8.94	0.43 ± 0.01
	15.9	5.01 ± 0.02	10.07 ± 0.01	0.413 ± 0.014	1037.40 ± 36.91	1163.89 ± 14.16	763.72 ± 10.25	1.41 ± 0.06
	31.9	4.21 ± 0.03	10.05 ± 0.02	0.407 ± 0.003	1218.12 ± 12.85	1566.60 ± 21.39	967.82 ± 15.87	2.99 ± 0.07
	47.8	3.86 ± 0.02	10.03 ± 0.02	0.407 ± 0.003	1333.21 ± 11.25	1812.76 ± 48.87	1034.86 ± 20.49	4.38 ± 0.25
	63.7	3.74 ± 0.01	10.02 ± 0.02	0.410 ± 0.002	1386.57 ± 8.37	1991.02 ± 41.28	1093.57 ± 30.89	5.50 ± 0.22
	79.6	3.63 ± 0.02	10.02 ± 0.03	0.408 ± 0.002	1425.20 ± 8.94	2062.31 ± 43.01	1137.93 ± 29.56	6.06 ± 0.24
HF01_HS	6.4	6.67 ± 0.02	10.07 ± 0.01	0.408 ± 0.001	766.47 ± 4.59	717.28 ± 7.41	519.47 ± 12.34	0.39 ± 0.01
	15.9	5.09 ± 0.01	10.07 ± 0.01	0.406 ± 0.002	1002.10 ± 4.52	1074.52 ± 7.50	721.99 ± 11.37	1.16 ± 0.02
	31.9	4.23 ± 0.02	10.04 ± 0.01	0.407 ± 0.002	1214.79 ± 6.80	1481.76 ± 19.25	911.64 ± 12.77	2.67 ± 0.08
	47.8	3.87 ± 0.01	10.02 ± 0.01	0.404 ± 0.001	1322.11 ± 2.17	1676.17 ± 19.08	1015.75 ± 21.85	3.71 ± 0.08
	63.7	3.74 ± 0.01	10.01 ± 0.01	0.408 ± 0.001	1383.25 ± 5367	1847.73 ± 24.72	1071.63 ± 29.52	4.72 ± 0.13
	79.6	3.66 ± 0.02	10.02 ± 0.01	0.408 ± 0.001	1417.41 ± 4.54	1946.37 ± 17.67	1133.13 ± 19.32	5.37 ± 0.09
HF02_LS	6.4	6.52 ± 0.03	10.10 ± 0.01	0.397 ± 0.001	761.01 ± 4.92	749.31 ± 8.13	535.74 ± 11.91	0.43 ± 0.01
	15.9	5.01 ± 0.01	10.07 ± 0.01	0.409 ± 0.003	1026.28 ± 6.78	1159.73 ± 16.32	771.96 ± 19.84	1.38 ± 0.04
	31.9	4.14 ± 0.02	10.04 ± 0.01	0.404 ± 0.002	1230.89 ± 9.83	1559.32 ± 16.91	967.29 ± 25.41	2.99 ± 0.07
	47.8	3.84 ± 0.01	10.02 ± 0.01	0.403 ± 0.003	1332.28 ± 10.25	1823.28 ± 36.94	1106.63 ± 19.44	4.43 ± 0.18
	63.7	3.68 ± 0.02	10.03 ±0.02	0.404 ± 0.002	1390.28 ± 7.95	1947.23 ± 72.41	1121.95 ± 22.14	5.28 ± 0.39
	79.6	3.62 ± 0.02	10.01 ± 0.02	0.406 ± 0.003	1422.78 ± 7.23	2145.65 ± 66.56	1175.32 ± 17.99	6.56 ± 0.40
HF02_HS	6.4	6.71 ± 0.02	10.07 ± 0.01	0.405 ± 0.003	785.60 ± 6.47	711.95 ± 6.89	520.96 ± 19.45	0.38 ± 0.01
	15.9	5.07 ± 0.01	10.05 ± 0.01	0.406 ± 0.002	1009.22 ± 7.26	1107.16 ± 14.06	741.23 ± 23.17	1.24 ± 0.03
	31.9	4.21 ± 0.01	10.04 ± 0.01	0.409 ± 0.002	1229.62 ± 7.37	1538.52 ± 23.53	950.34 ± 15.47	2.91 ± 0.09
	47.8	3.85 ± 0.02	10.03 ± 0.01	0.406 ± 0.003	1335.50 ± 7.58	1743.90 ± 30.14	1066.48 ± 14.97	4.06 ± 0.15
	63.7	3.73 ± 0.01	10.01 ± 0.01	0.409 ± 0.002	1395.29 ± 5.26	1902.23 ± 45.49	1120.12 ± 21.59	5.05 ± 0.25
	79.6	3.60 ± 0.02	10.01 ± 0.01	0.405 ± 0.002	1429.64 ± 4.29	2031.71 ± 27.86	1168.82 ± 18.94	5.90 ± 0.15
HF03_LS	6.4	6.45 ± 0.01	10.07 ± 0.01	0.397 ± 0.001	771.84 ± 3.59	755.37 ± 7.75	527.82 ± 15.44	0.44 ± 0.01
	15.9	4.96 ± 0.02	10.05 ± 0.01	0.405 ± 0.001	1028.81 ± 3.78	1168.26 ± 32.75	746.98 ± 12.39	1.41 ± 0.08
	31.9	4.09 ± 0.01	10.04 ± 0.01	0.401 ± 0.001	1240.30 ± 5.27	1576.60 ± 20.31	931.66 ± 23.12	3.08 ± 0.08
	47.8	3.80 ± 0.02	10.02 ± 0.01	0.403 ± 0.001	1344.35 ± 4.56	1820.16 ± 28.16	1035.42 ± 19.62	4.45 ± 0.14
	63.7	3.69 ± 0.01	10.02 ± 0.01	0.407 ± 0.002	1401.30 ± 3.91	1973.20 ± 45.48	1094.96 ± 21.11	5.46 ± 0.26
	79.6	3.62 ± 0.01	10.01 ± 0.01	0.409 ± 0.002	1433.50 ± 4.32	2149.45 ± 66.75	1134.79 ± 14.95	6.63 ± 0.41
HF03_HS	6.4	6.39 ± 0.01	10.05 ± 0.01	0.397 ± 0.001	782.33 ± 3.45	743.50 ± 4.75	531.61 ± 23.14	0.43 ± 0.01
	15.9	5.05 ± 0.01	10.04 ± 0.01	0.406 ± 0.001	1015.47 ± 3.95	1125.40 ± 5.67	713.27 ± 14.56	1.29 ± 0.01
	31.9	4.16 ± 0.01	10.03 ± 0.01	0.403 ± 0.001	1229.12 ± 6.20	1514.37 ± 15.68	898.19 ± 23.19	2.82 ± 0.06
	47.8	3.82 ± 0.01	10.02 ± 0.01	0.405 ± 0.001	1346.49 ± 3.73	1715.83 ± 16.25	997.38 ± 19.17	3.96 ± 0.08
	63.7	3.67 ± 0.03	10.01 ± 0.01	0.405 ± 0.001	1402.02 ± 11.19	1841.36 ± 46.03	1063.77 ± 22.54	4.76 ± 0.21
	79.6	3.62 ± 0.02	10.00 ± 0.01	0.408 ± 0.001	1439.07 ± 4.76	1908.17 ± 36.94	1096.97 ± 19.87	5.24 ± 0.22
HF04_LS	6.4	6.36 ± 0.02	10.05 ± 0.01	0.397 ± 0.002	786.30 ± 3.79	777.82 ± 4.18	544.52 ± 21.98	0.48 ± 0.01
	15.9	4.87 ± 0.01	10.05 ± 0.01	0.404 ± 0.001	1045.64 ± 5.39	1197.63 ± 16.64	770.57 ± 19.21	1.50 ± 0.04
	31.9	4.08 ± 0.01	10.03 ± 0.01	0.404 ± 0.001	1254.38 ± 5.41	1626.92 ± 34.94	946.64 ± 21.97	3.32 ± 0.15
	47.8	3.79 ± 0.01	10.02 ± 0.01	0.405 ± 0.001	1355.54 ± 3.28	1915.53 ± 87.34	1044.08 ± 15.21	4.98 ± 0.48
	63.7	3.62 ± 0.01	10.02 ± 0.01	0.403 ± 0.001	1410.73 ± 7.30	2081.19 ± 83.10	1120.74 ± 25.54	6.12 ± 0.48
	79.6	3.55 ± 0.01	10.01 ± 0.01	0.404 ± 0.001	1443.91 ± 3.03	2158.55 ± 68.73	1130.57 ± 12.17	6.73 ± 0.43
HF04_HS	6.4	6.45 ± 0.02	10.03 ± 0.01	0.400 ± 0.001	784.23 ± 5.06	749.50 ± 4.53	534.38 ± 21.11	0.44 ± 0.01
	15.9	4.91 ± 0.04	10.03 ± 0.01	0.403 ± 0.001	1036.84 ± 8.24	1163.53 ± 16.65	758.89 ± 18.34	1.40 ± 0.04
	31.9	4.09 ± 0.01	10.01 ± 0.01	0.405 ± 0.001	1257.70 ± 4.88	1568.08 ± 20.39	995.13 ± 23.17	3.09 ± 0.08
	47.8	3.81 ± 0.02	10.01 ± 0.01	0.405 ± 0.002	1352.92 ± 6.61	1784.10 ± 43.76	1079.32 ± 12.14	4.31 ± 0.21
	63.7	3.66 ± 0.02	10.00 ± 0.01	0.405 ± 0.001	1407.05 ± 4.78	1915.94 ± 18.75	1119.27 ± 13.29	5.17 ± 0.10
	79.6	3.59 ± 0.02	9.99 ± 0.01	0.406 ± 0.003	1441.31 ± 6.68	1939.59 ± 28.61	1165.58 ± 19.47	5.42 ± 0.16
HF05_LS	6.4	6.43 ± 0.05	10.05 ± 0.02	0.389 ± 0.027	763.71 ± 54.74	770.32 ± 7.68	515.22 ± 21.15	0.45 ± 0.03
	15.9	4.92 ± 0.01	10.06 ± 0.01	0.404 ± 0.001	1032.06 ± 3.91	1162.29 ± 20.59	725.66 ± 19.45	1.39 ± 0.05
	31.9	4.06 ± 0.01	10.03 ± 0.01	0.402 ± 0.002	1253.83 ± 3.51	1615.65 ± 32.60	937.64 ± 17.75	3.27 ± 0.13
	47.8	3.79 ± 0.01	10.02 ± 0.01	0.404 ± 0.001	1354.47 ± 4.36	1817.41 ± 22.23	1044.08 ± 22.51	4.47 ± 0.11
	63.7	3.65 ± 0.01	10.01 ± 0.01	0.406 ± 0.001	1411.76 ± 3.64	1967.27 ± 36.33	1079.88 ± 14.36	5.47 ± 0.19
	79.6	3.59 ± 0.01	10.01 ± 0.01	0.408 ± 0.001	1442.86 ± 5.87	2029.87 ± 36.24	1132.49 ± 15.14	5.95 ± 0.21
HF05_HS	6.4	6.51 ± 0.01	10.04 ± 0.01	0.400 ± 0.002	776.02 ± 3.71	735.65 ± 5.42	513.81 ± 14.23	0.42 ± 0.01
	15.9	4.92 ± 0.01	10.03 ± 0.01	0.401 ± 0.001	1030.21 ± 4.13	1142.20 ± 9.15	738.74 ± 23.17	1.34 ± 0.02
	31.9	4.13 ± 0.01	10.01 ± 0.01	0.406 ± 0.001	1247.37 ± 3.71	1526.26 ± 11.37	909.69 ± 19.78	2.91 ± 0.05
	47.8	3.78 ± 0.01	10.01 ± 0.01	0.403 ± 0.001	1358.08 ± 4.08	1740.22 ± 26.82	1008.15 ± 11.12	4.11 ± 0.13
	63.7	3.64 ± 0.02	10.00 ± 0.01	0.404 ± 0.001	1415.32 ± 5.97	1816.42 ± 35.61	1073.75 ± 14.38	4.67 ± 0.19
	79.6	3.56 ± 0.02	10.00 ± 0.02	0.403 ± 0.003	1441.48 ± 6.97	1898.01 ± 48.87	1109.03 ± 18.74	5.20 ± 0.27

26

HF01
No Head
Flat

HF02
50% Head
Flat

HF03
Standard Head
Flat

HF04
Extended Head
Flat

HF05
0.625 Head
Flat

Fig. 1.a
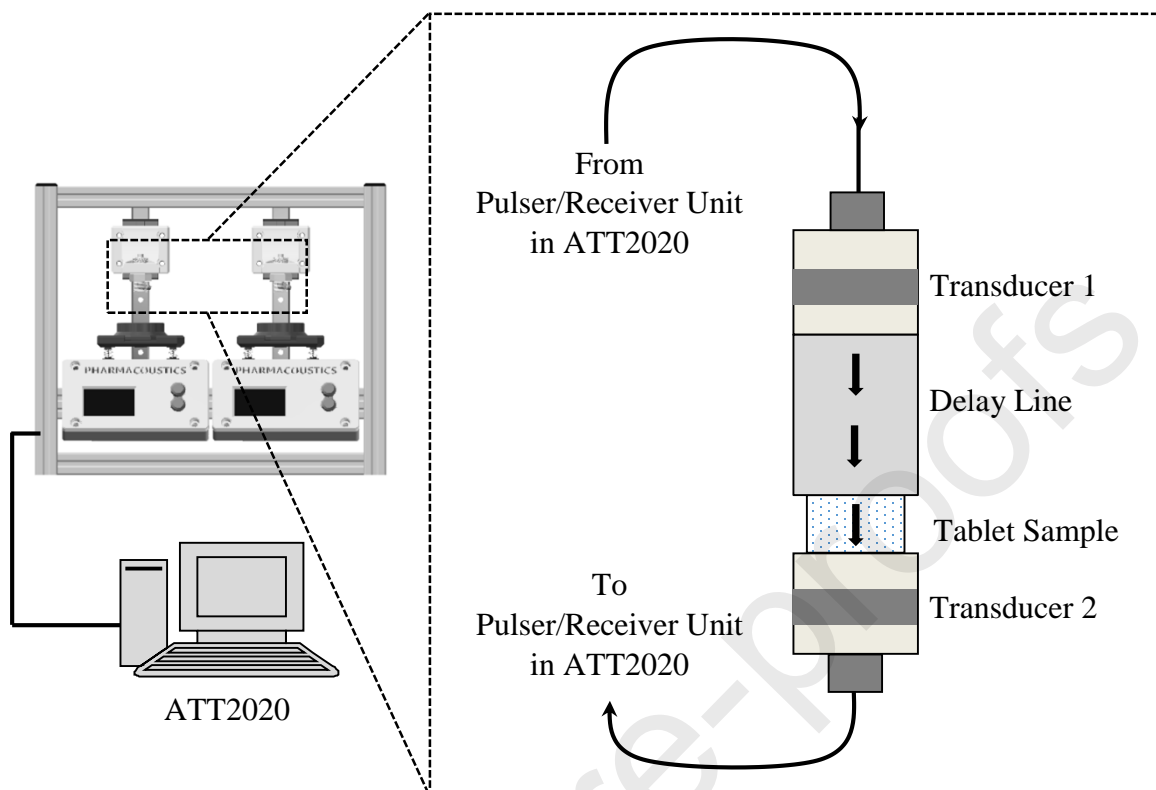
Fig. 1.b

Figure 1. (*a*) Images of the head flats (top geometries indicated by dark cycles) (No HF, 50% HF, Standard HF, Extended HF, and 0.625 HF, respectively) of the upper punches utilized to prepare the compacts. (*b*) Schematic of the experimental rig operating in the pitch-catch mode.

Figure 2.a

29
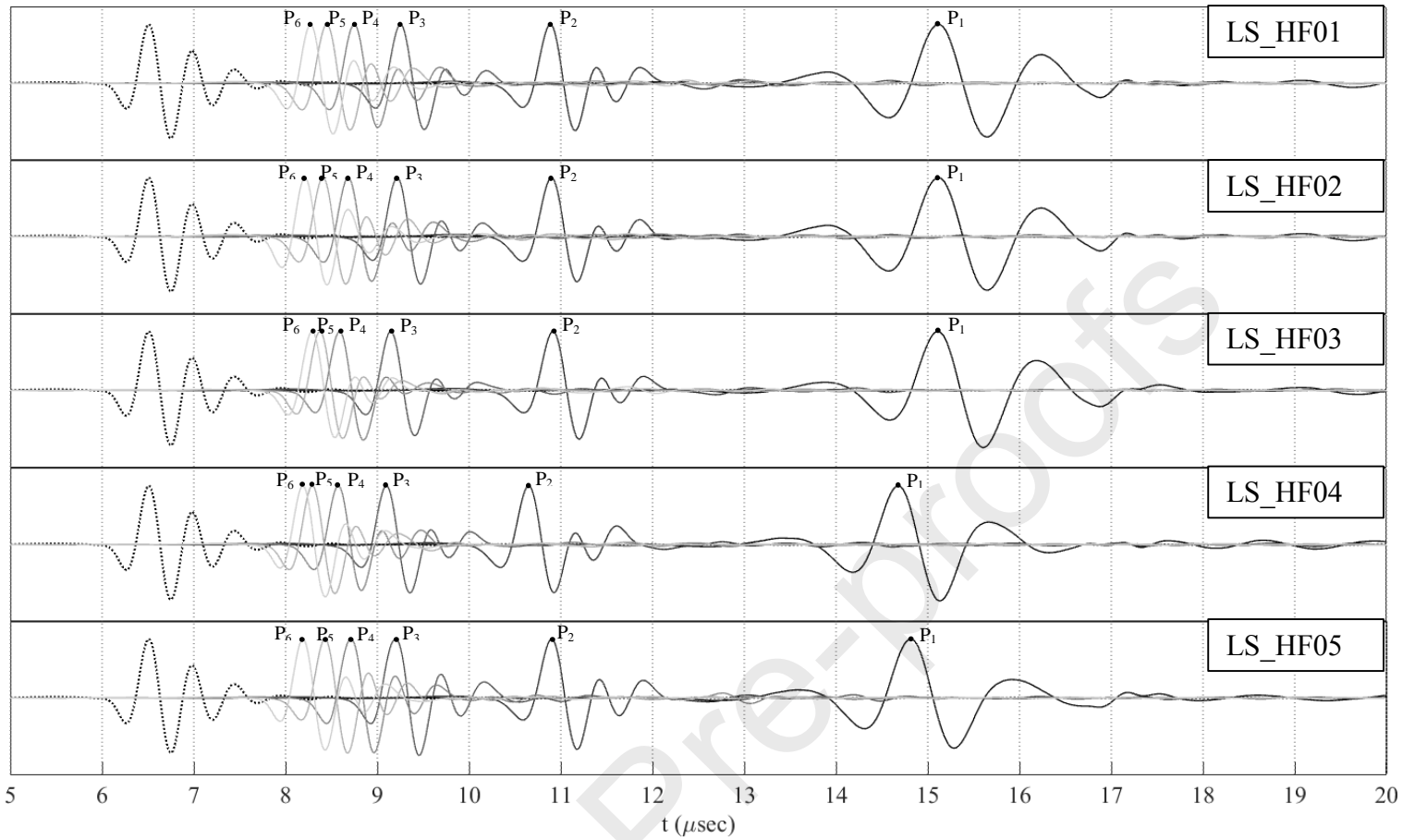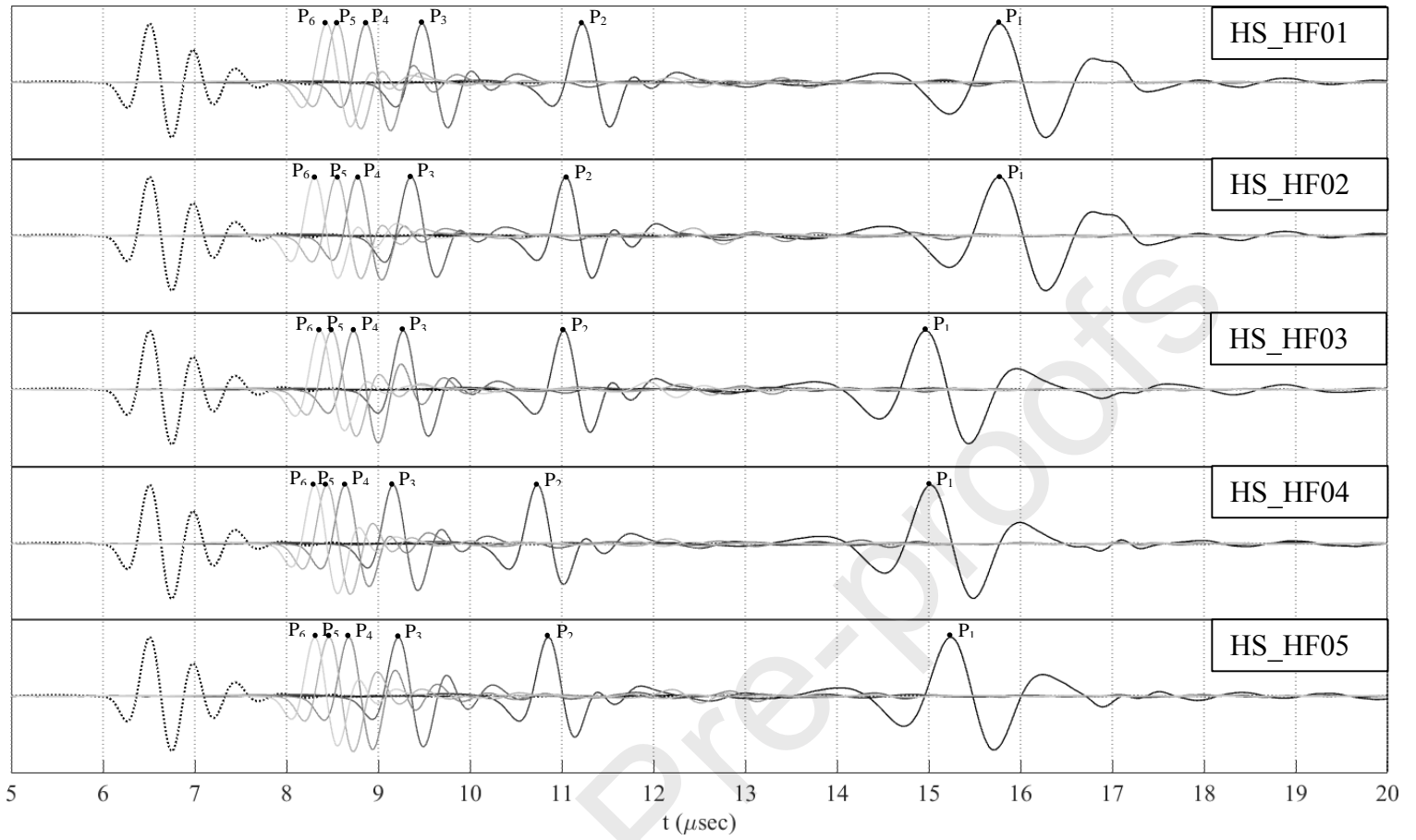
Fig. 2.b
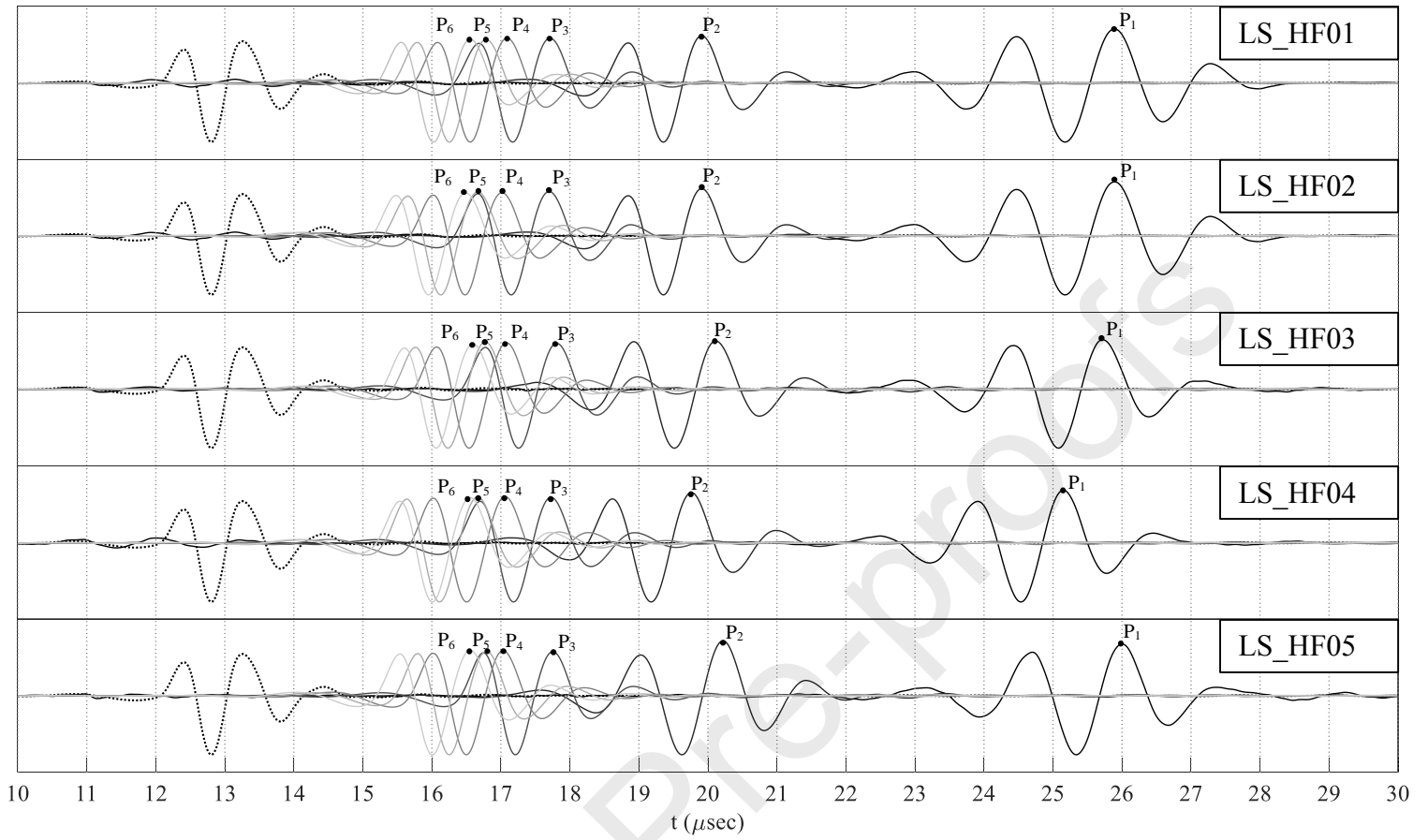
Fig. 2.c
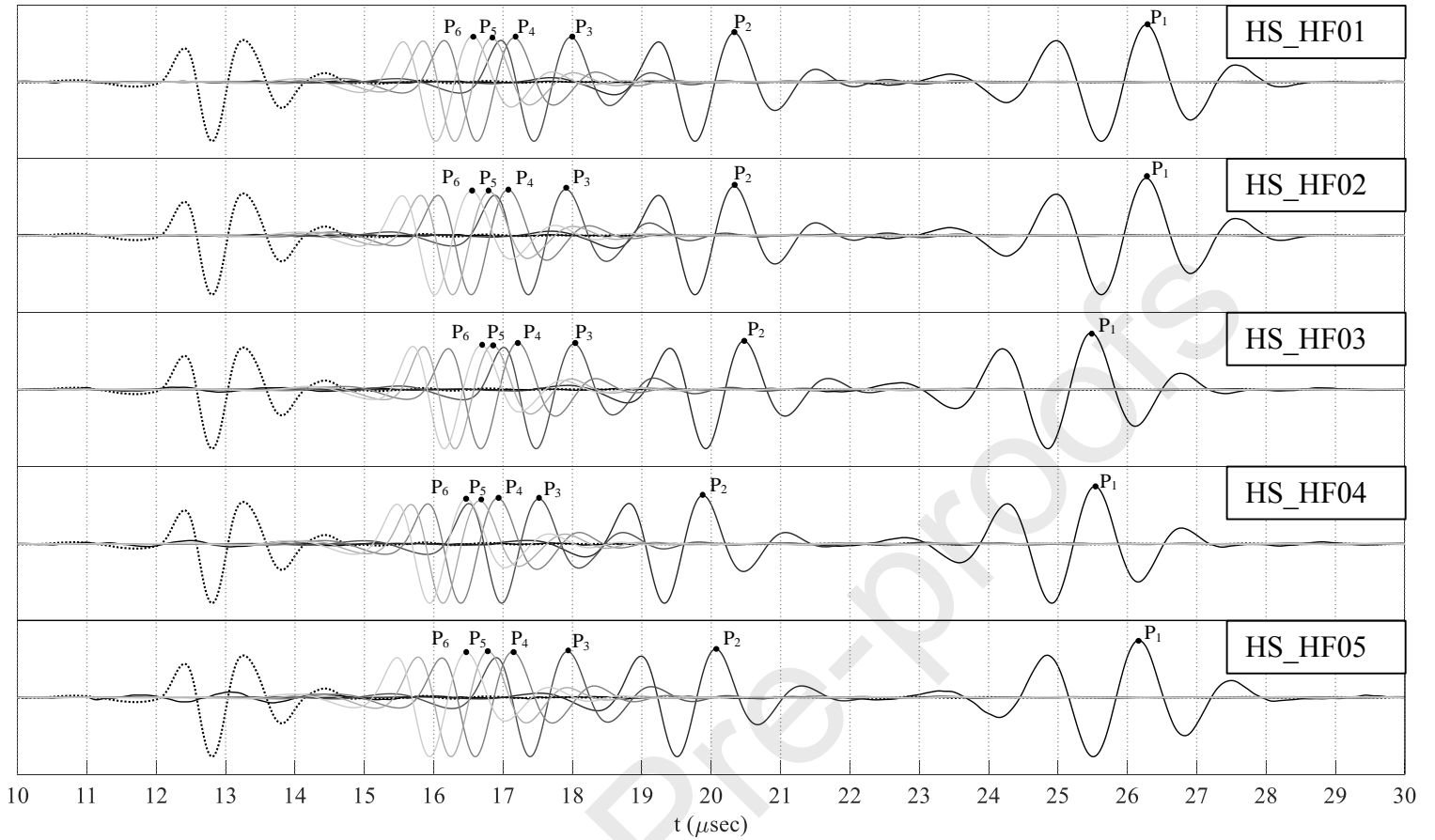
Fig. 2.d

Figure 2. Normalized propagating pressure (*a-b*) and shear (*c-d*) waveforms for low compaction speed (LS) with a dwell-time of 4ms and high compaction speed (HS) with a dwell-time of 20ms for the five punch sets (HF01, HF02, HF03, HF04 and HF05) with the delay line waveform (dotted) at corresponding P_c (P_1 = 6.4 MPa, P_2 = 15.9MPa, P_3 =31.9MPa, P_4 =47.8MPa, P_5 =63.7MPa and P_6 = 79.6MPa).

Fig. 3.a

P_c (MPa)	LS	HS
P_1	○	●
P_2	△	▲
P_3	□	■
P_4	◇	◆
P_5	▽	▼
P_6	⊗	⊗
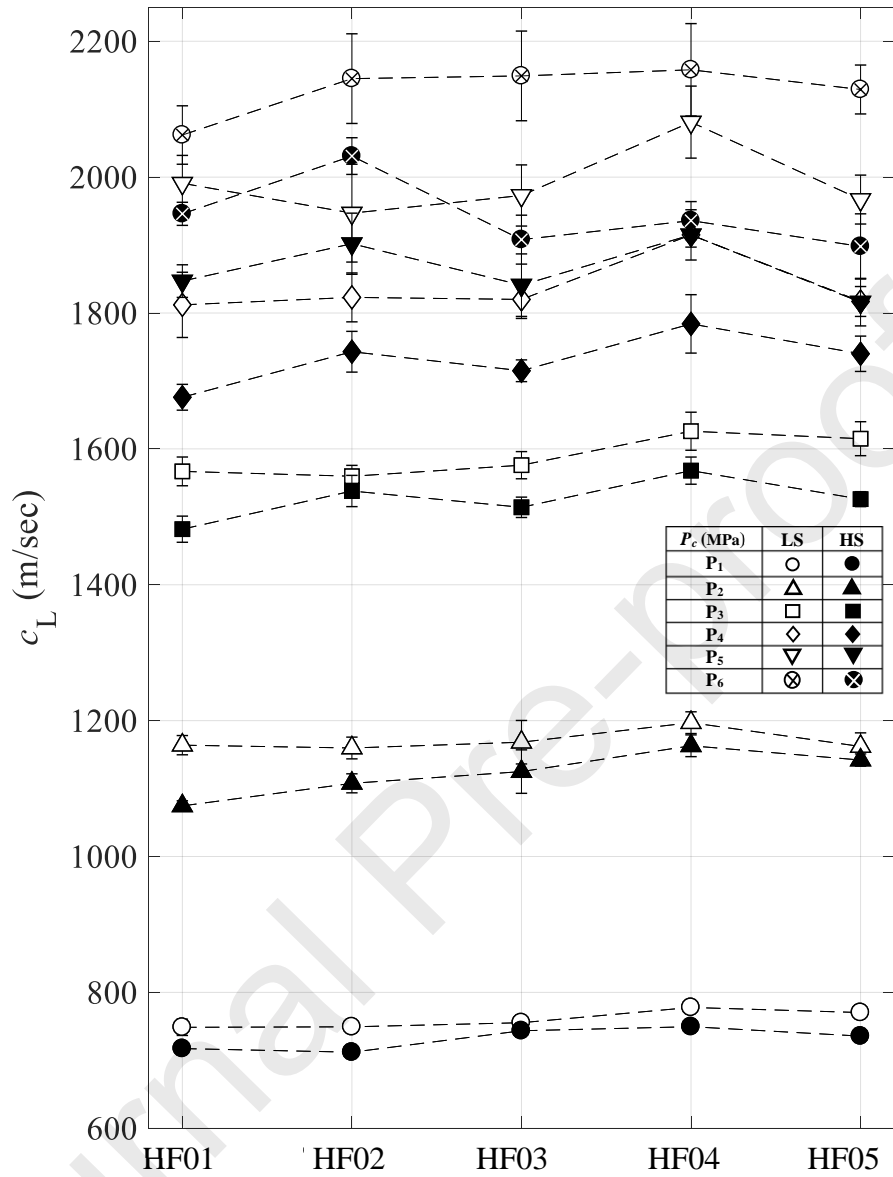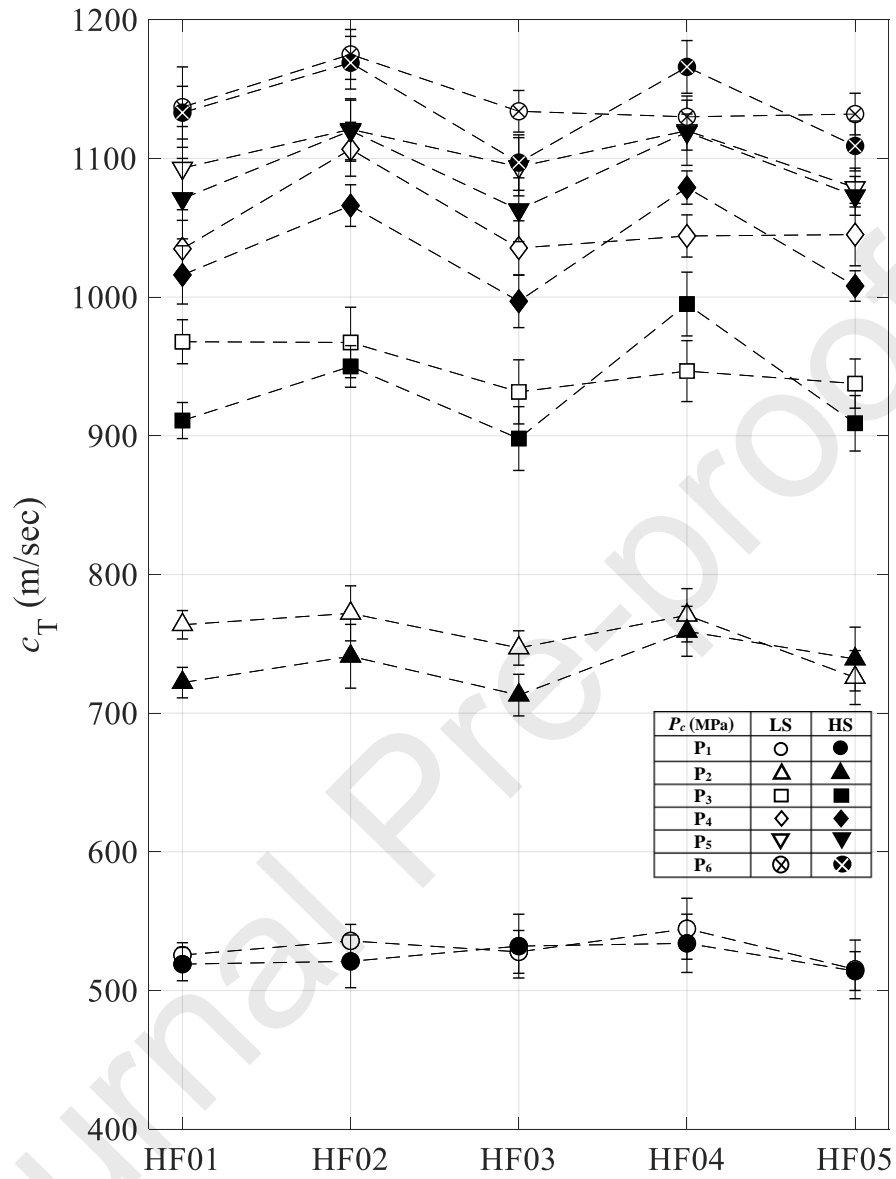
Fig. 3.b
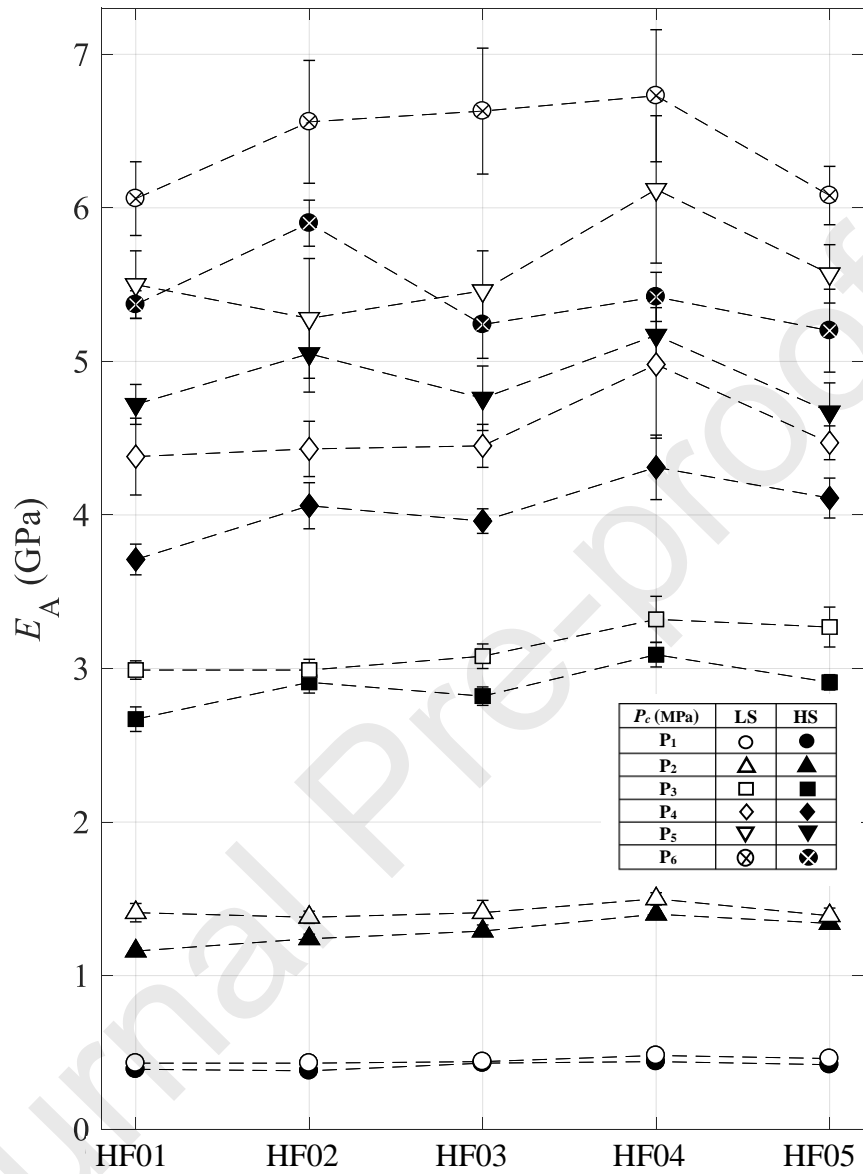
Fig. 3.c

Figure 3. Relationship between P_c and (*a*) pressure (c_L), (*b*) shear (c_T) and (*c*) Young's moduli (E_A) for the five punch sets (HF01, HF02, HF03, HF04 and HF05).

Compressibility of Prosolv® SMCC 90LM at low speed (20 RPM)

Legend:
- HF01
- HF02
- HF03
- HF04
- HF05

x-axis: P_c (MPa)

y-axis: ϕ^m (%)
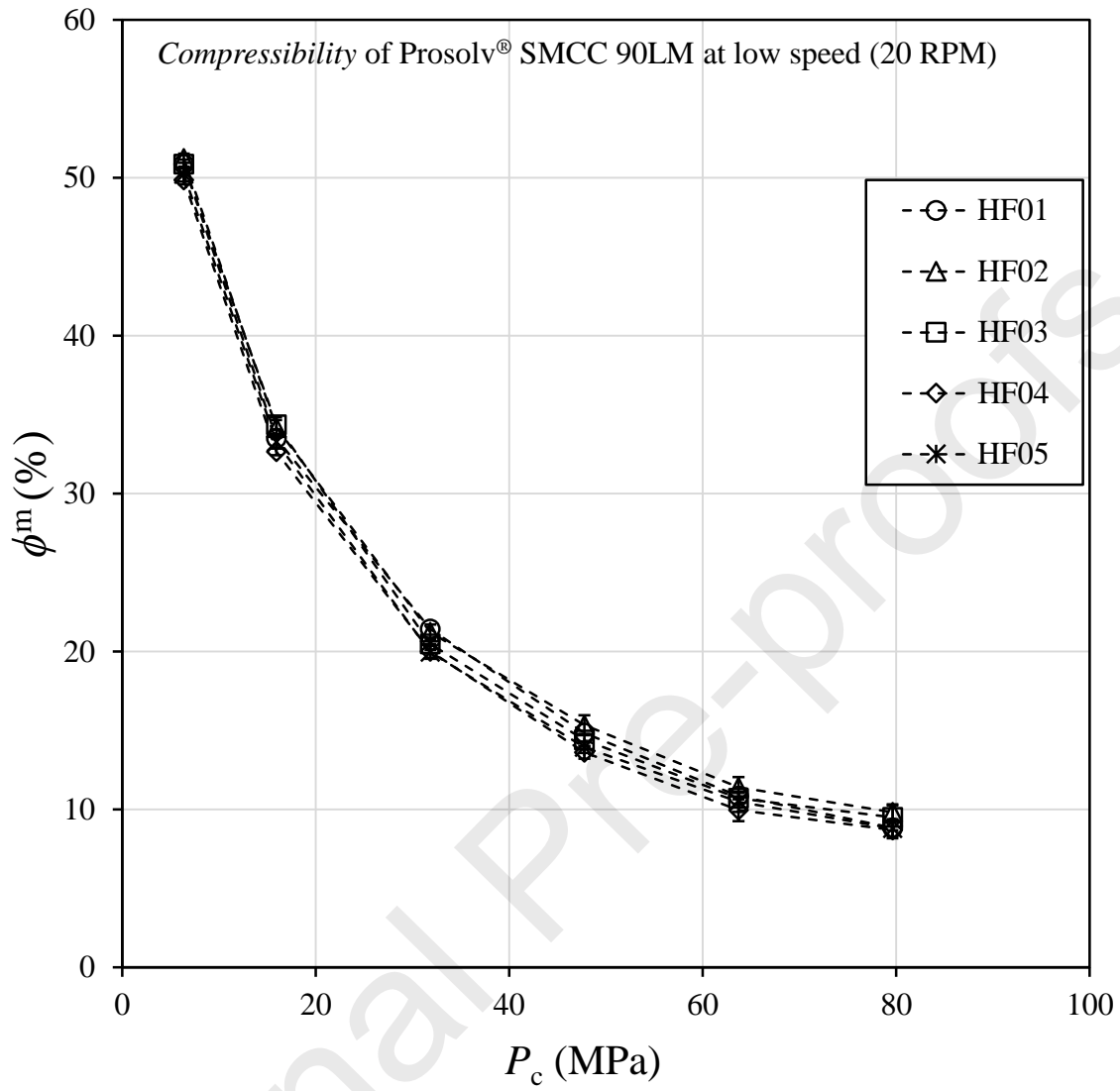
Fig. 4.a
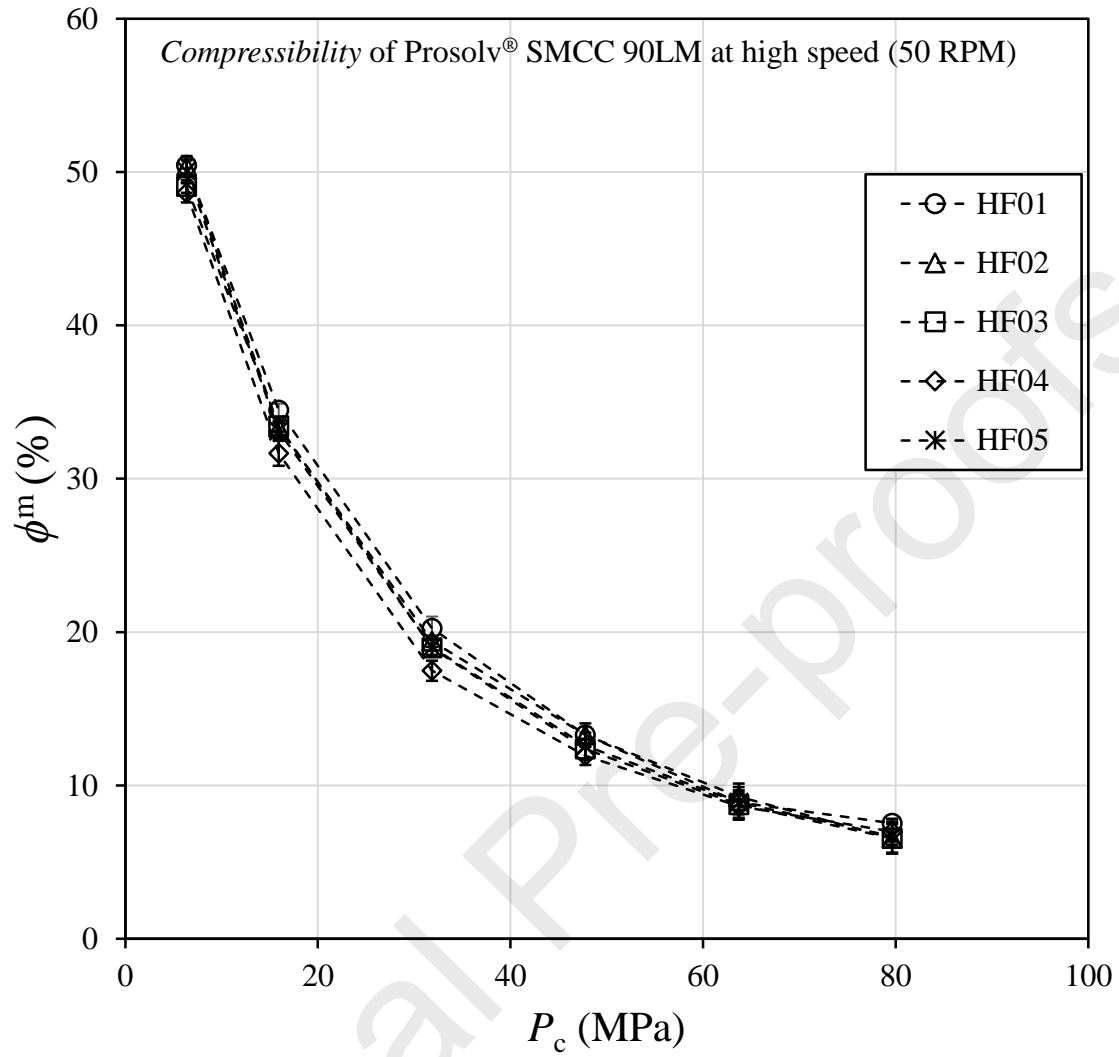
Fig. 4.b
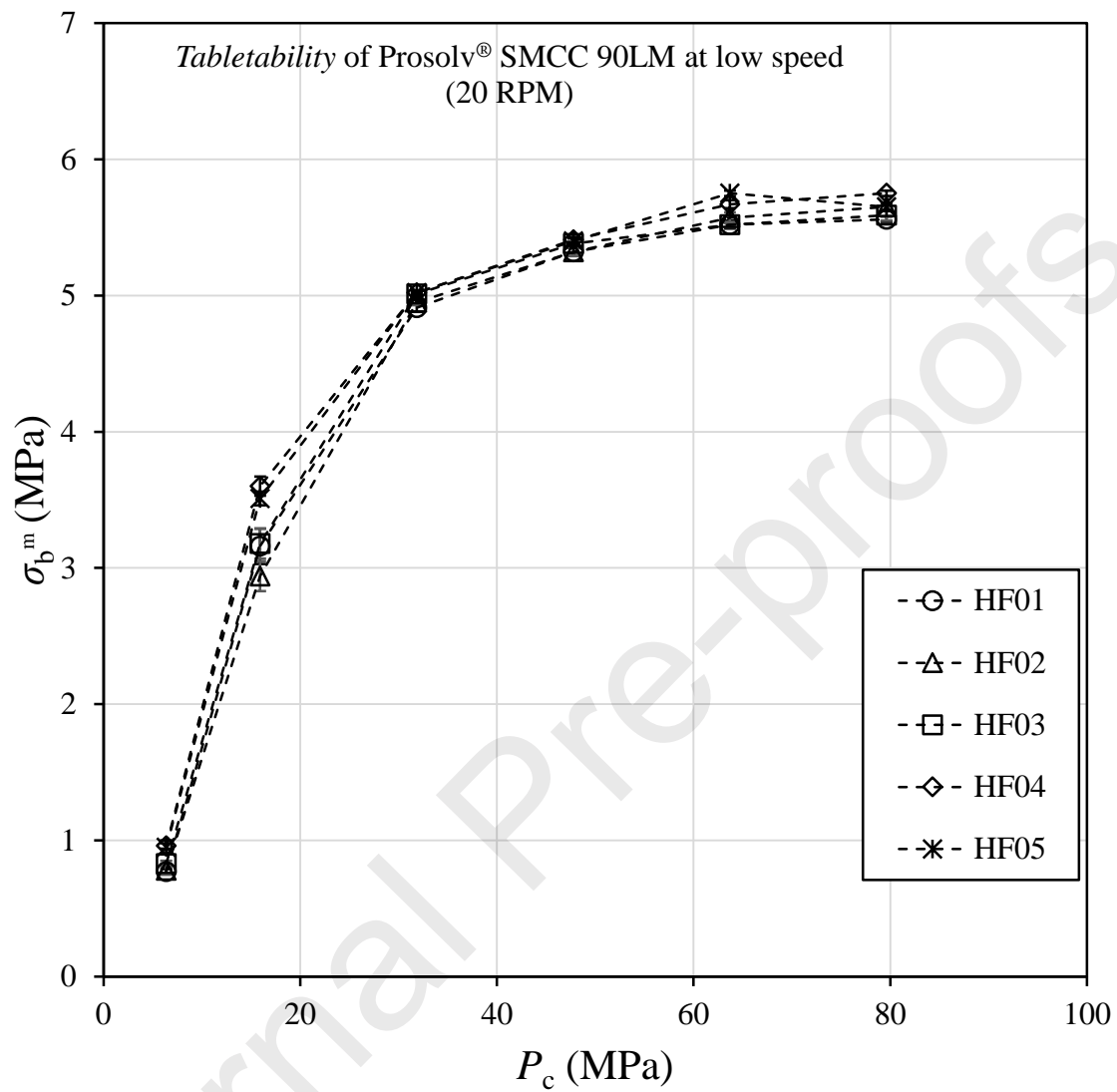
Fig. 4.c
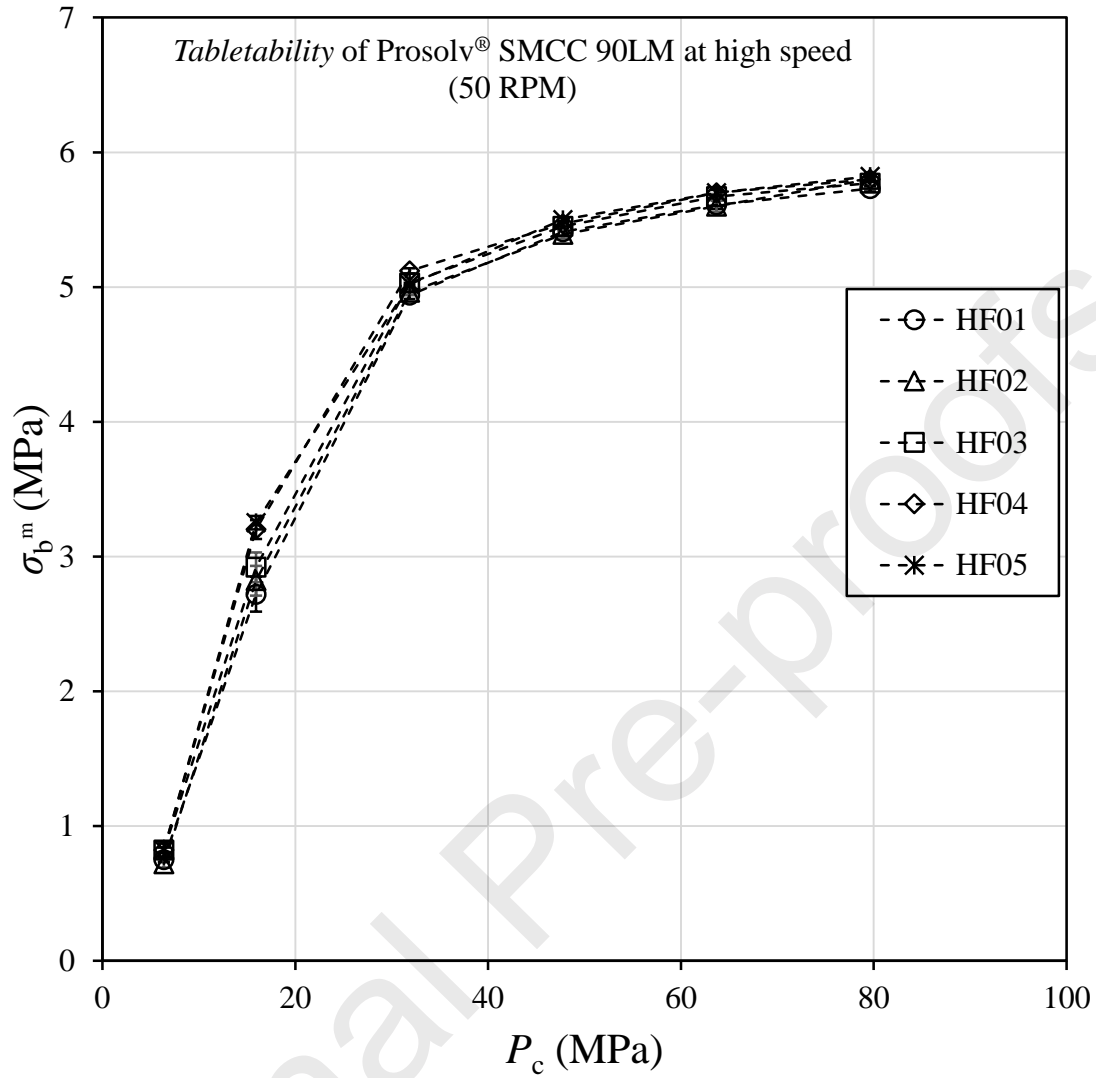
Fig. 4.d

Figure 4. Compressibility and tabletability data: Relationship between P_c and the measured

parameters: porosity ratio (ϕ^m) of (*a*) low compaction speed (LS), (*b*) high compaction speed (HS)

and tensile strength (σ_b^m) of (*c*) low compaction speed (LS), and (*d*) high compaction speed (HS)

for the five sample sets.
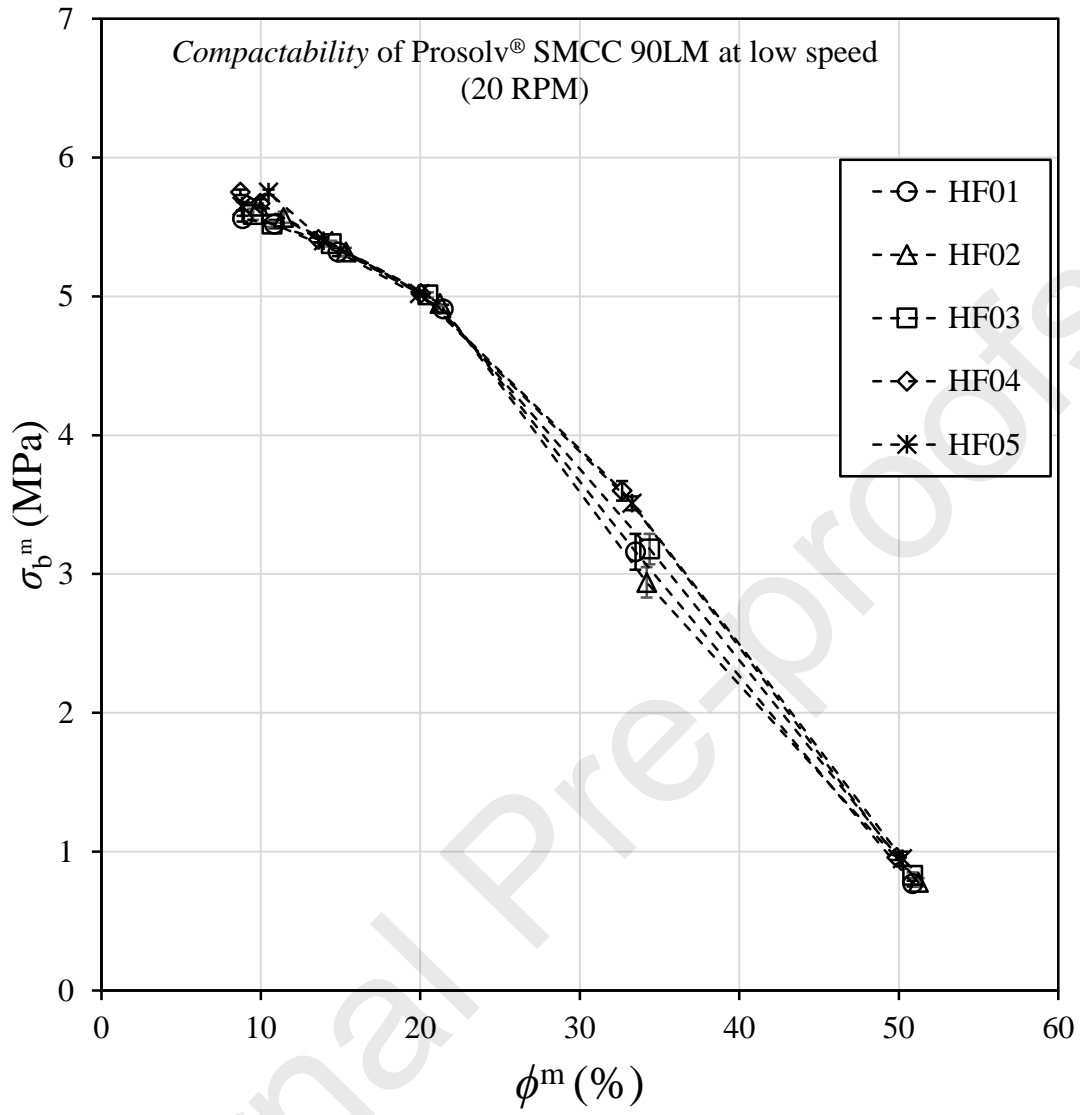
Fig. 5.a
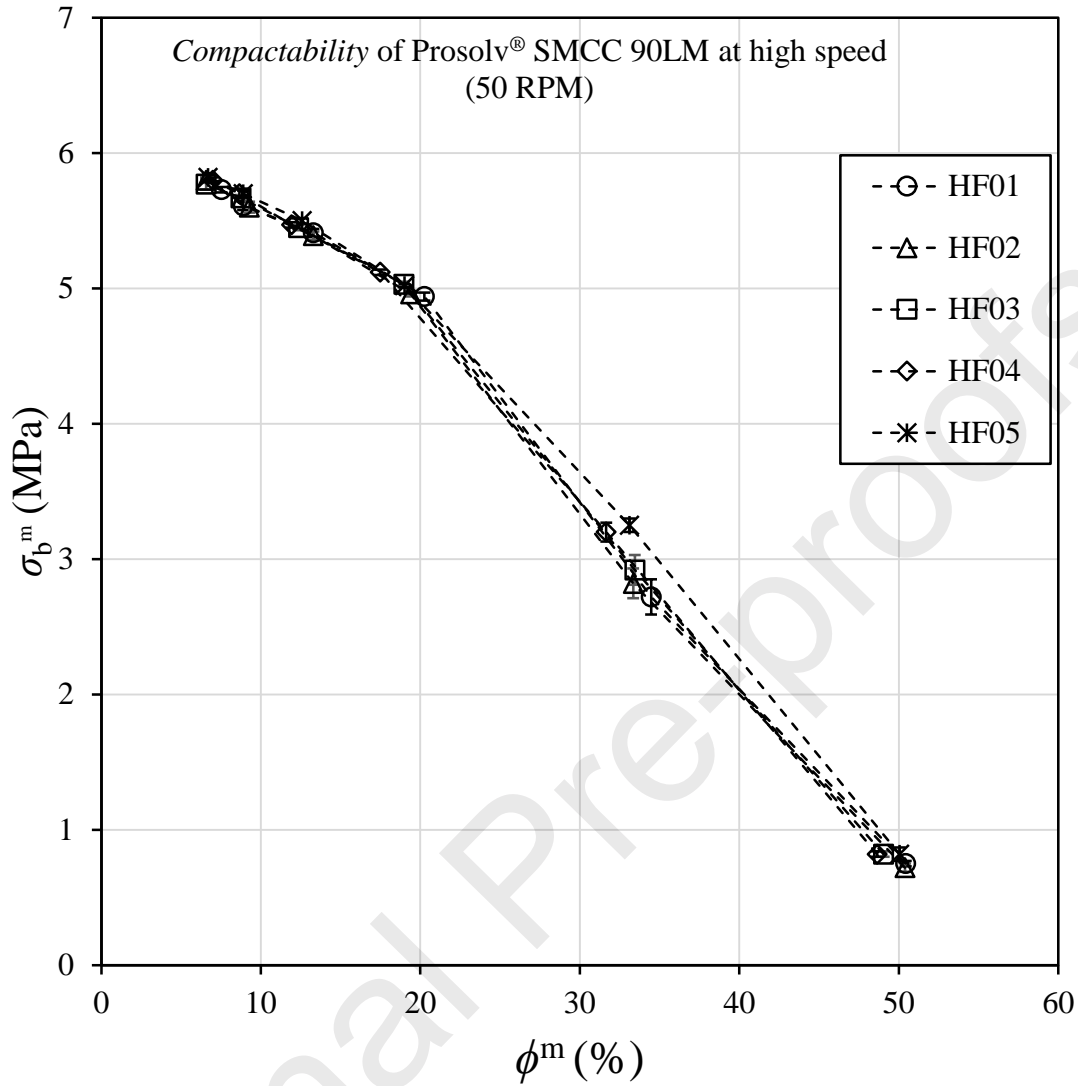
Fig. 5.b

Figure 5. Compactability data: relationship between the measured ϕ^m and σ_b^m of (*a*) low compaction speed and (*b*) high compaction speed for the five punch sets.
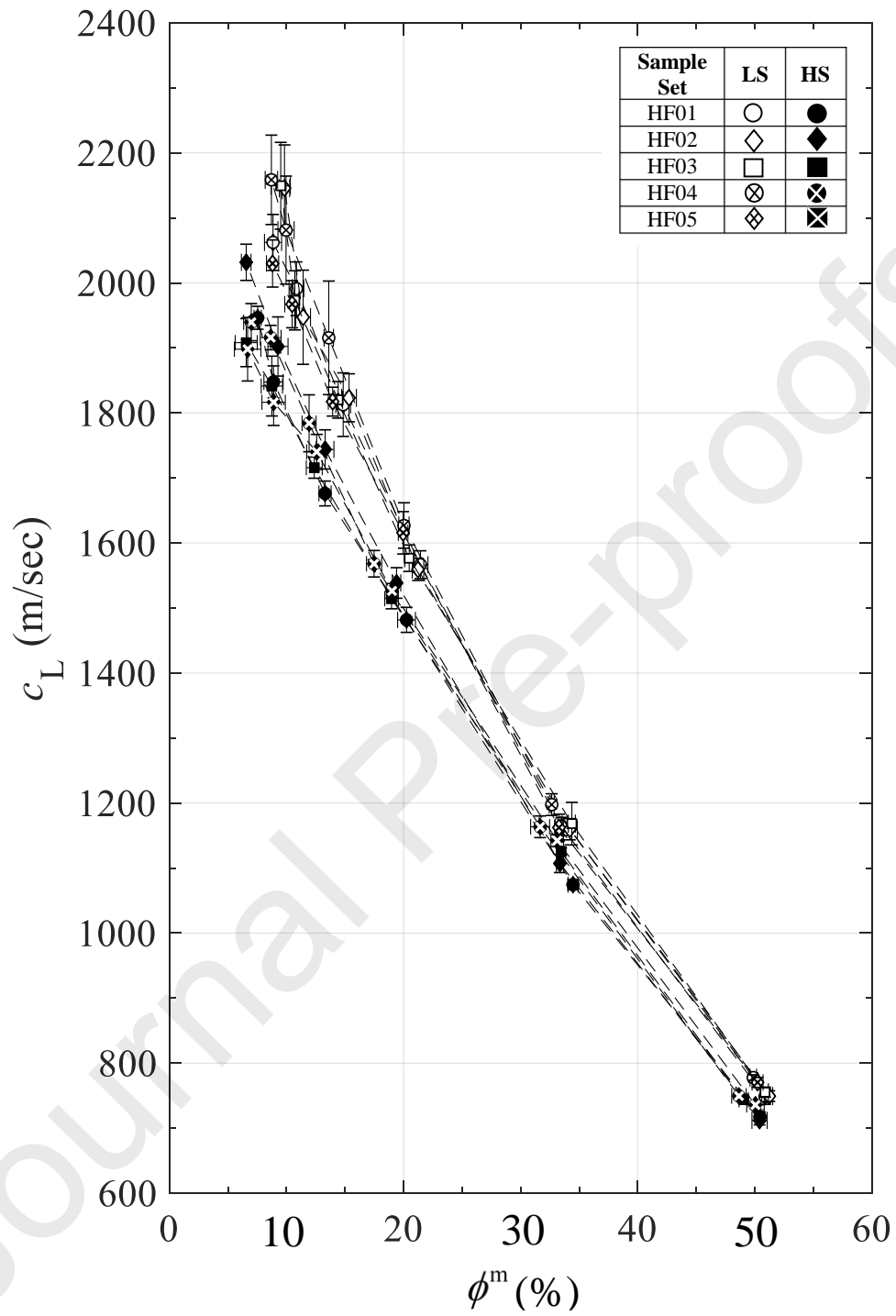
Fig. 6.a
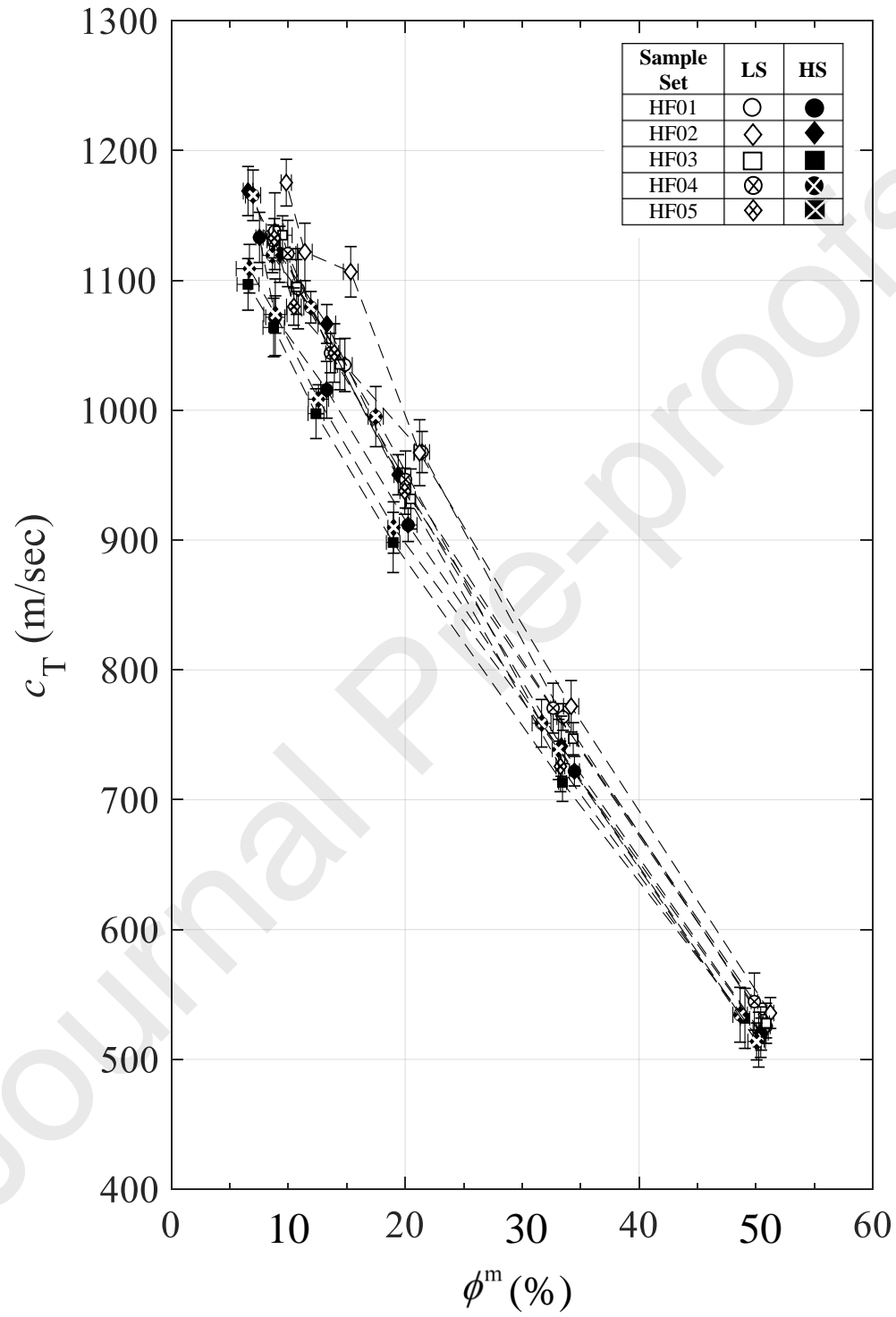
Fig. 6.b
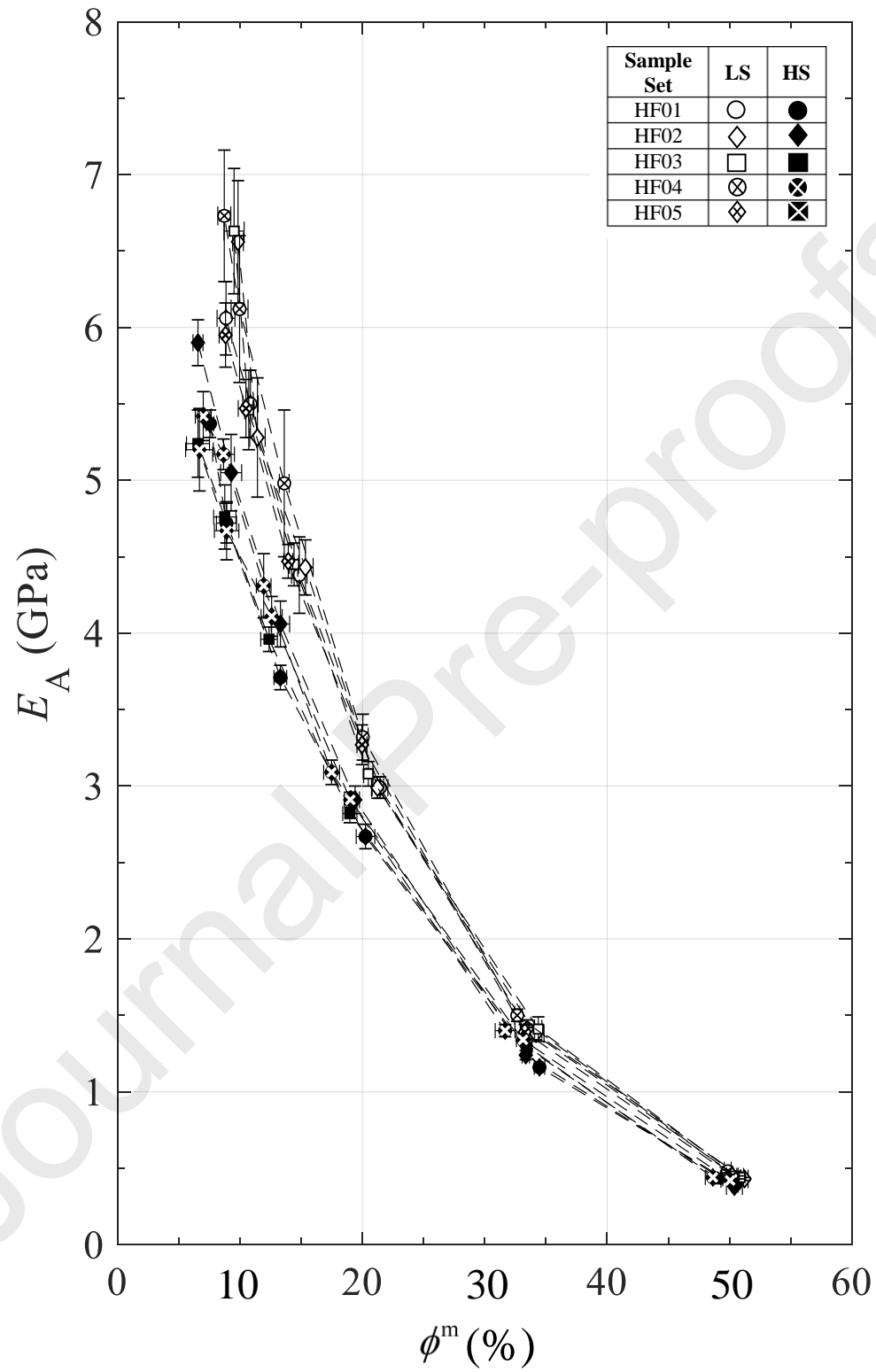
Fig. 6.c

Figure 6. Relationships between the measured ϕ^{m} and acoustically determined mechanical properties: (*a*) c_{L}, (*b*) c_{T}, and (*c*) E_{A} (extracted) for the five punch sets.

Fig. 7.a

Fig. 7.b

Sample Set	LS	HS
HF01	○	●
HF02	◇	◆
HF03	□	■
HF04	⊗	⊗
HF05	◈	⊠
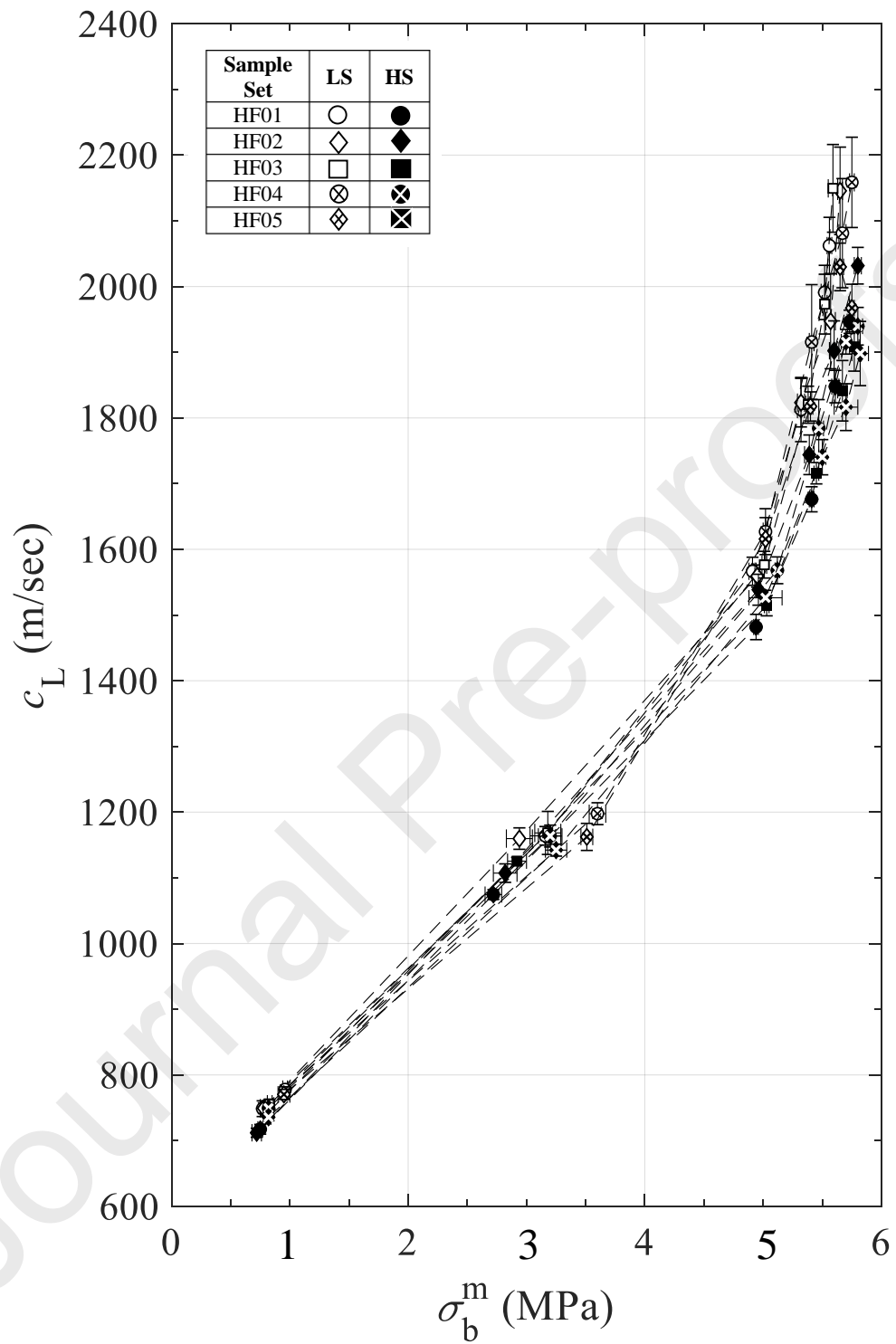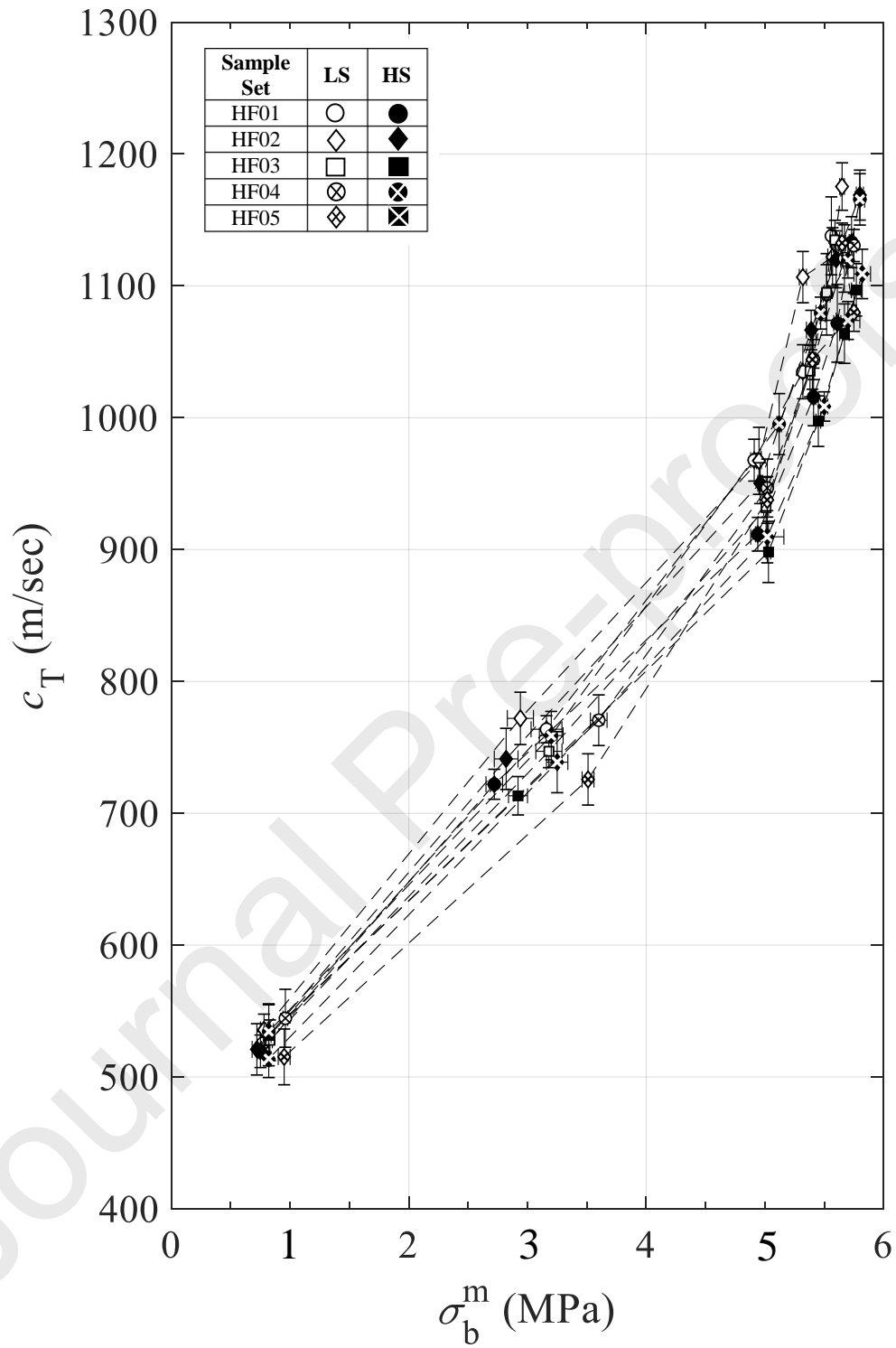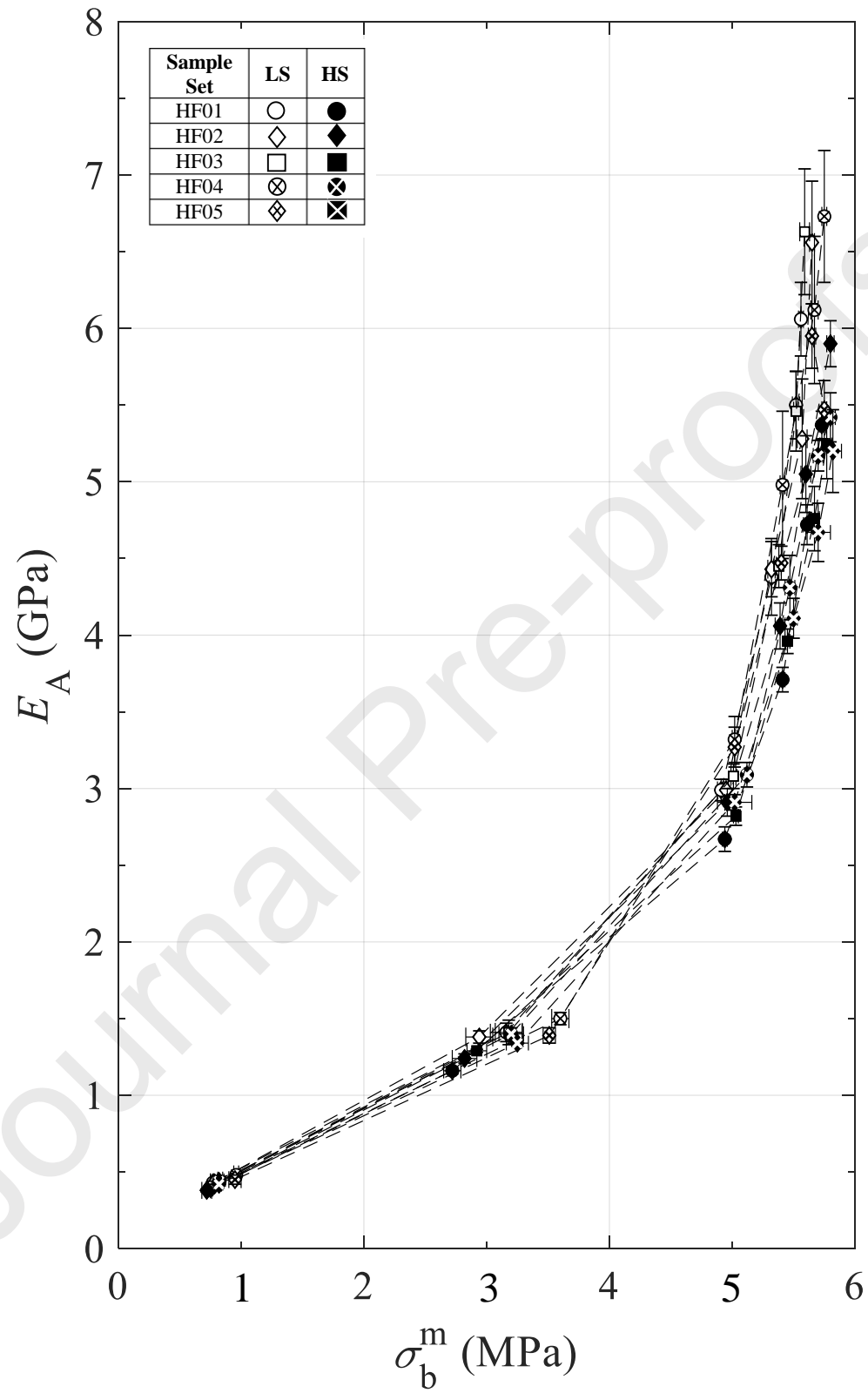
Fig. 7.c

Figure 7. Relationships between the measured σ_b^m and acoustically determined mechanical properties: (*a*) c_L, (*b*) c_T and (*c*) E_A (extracted) for the five punch sets.

Graphical abstract

Authors: *Xiaochi Xu, Yigitcan Coskunturk, Vivek S Dave, Justin V Kuriyilel, Murray F Wright, Rutesh H Dave, Cetin Cetinkaya.*

Date: *December 17, 2019*

CRediT author statement

Xiaochi Xu, Yigitcan Coskunturk: Formal analysis, Investigation, Writing - Review & Editing, Data Curation

Vivek S. Dave: Methodology, Formal analysis, Writing - Review & Editing, Supervision, Data Curation

Rutesh H. Dave: Resources, Supervision

Justin V. Kuriyilel, Murray F. Wright: Formal analysis, Investigation,

Cetin Cetinkaya: Conceptualization, Methodology, Software, Writing - Review & Editing, Supervision

52

Declaration of interests

☒ The authors declare that they have no known competing financial interests or personal relationships that could have appeared to influence the work reported in this paper.

☐The authors declare the following financial interests/personal relationships which may be considered as potential competing interests: